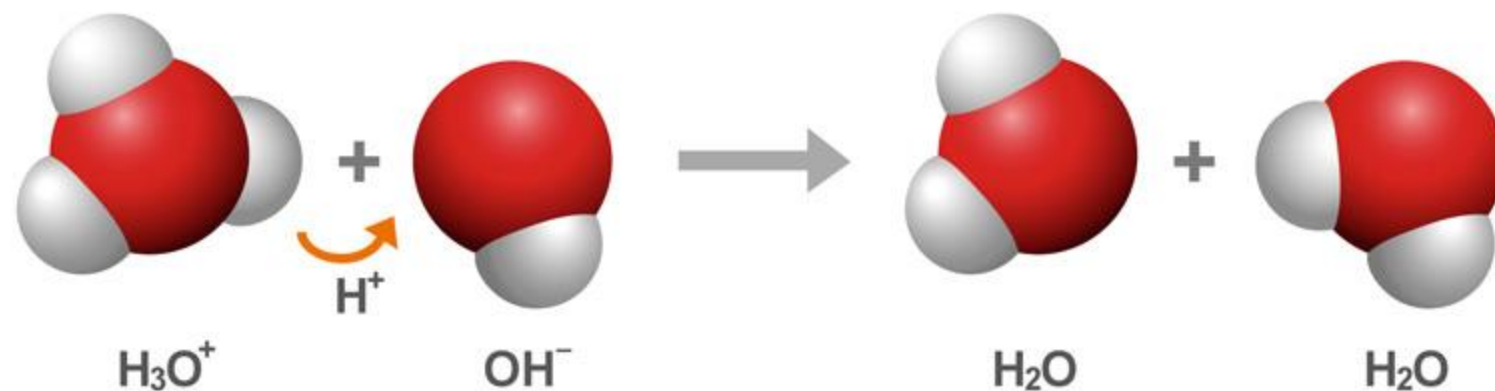
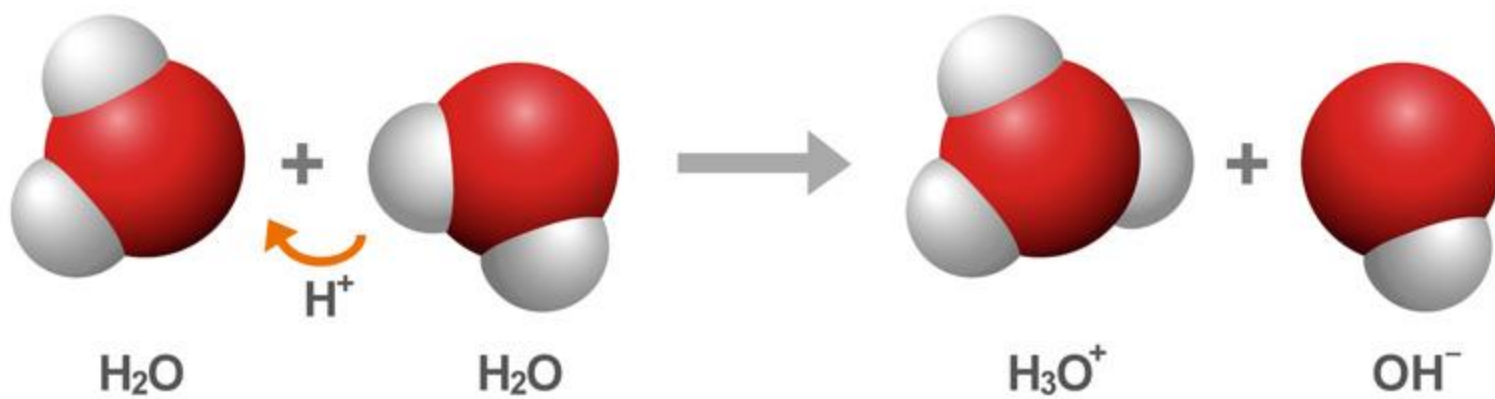


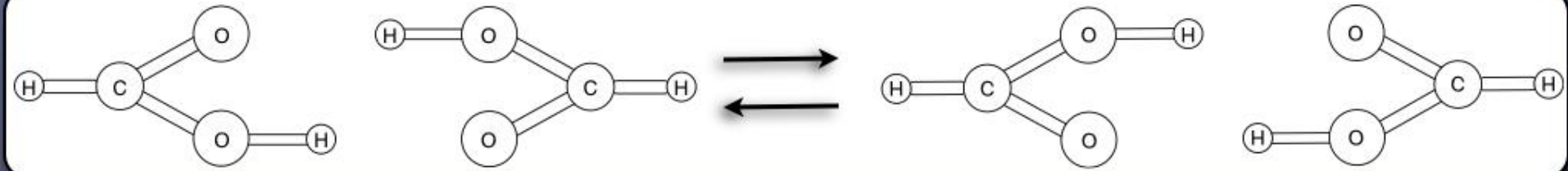
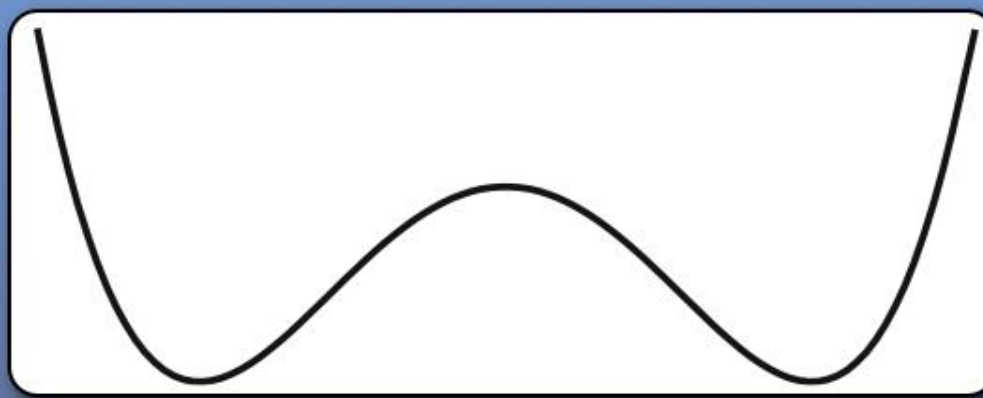


TSTC Dynamics Lectures
Proton Transfer and More
July 14-20

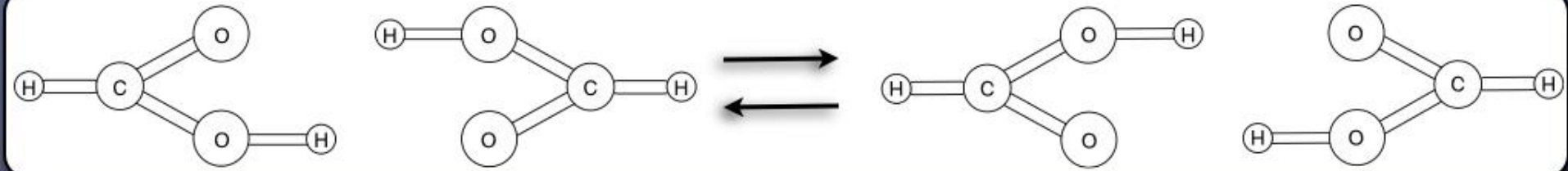
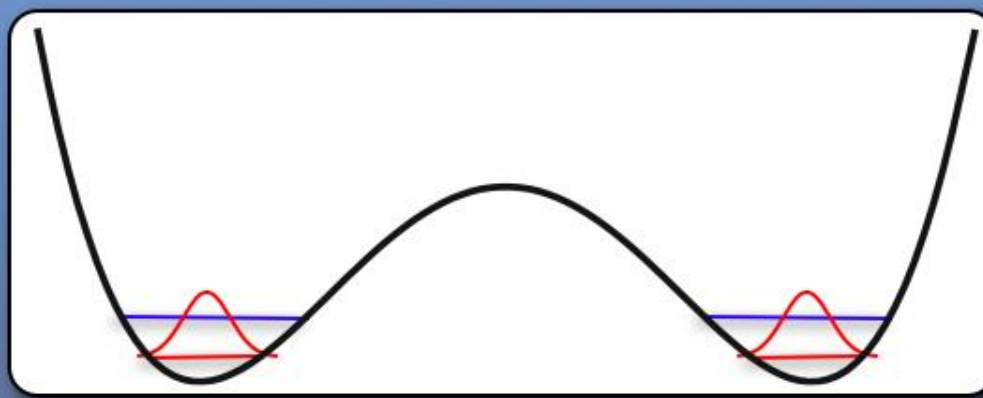
Ned Sibert
University of Wisconsin



Formic Acid Dimer



Formic Acid Dimer



Proton Transfer in Condensed Phase

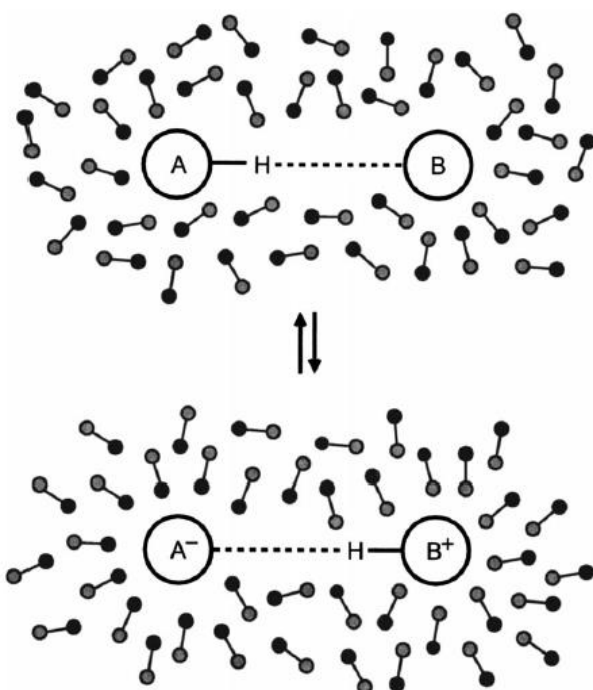
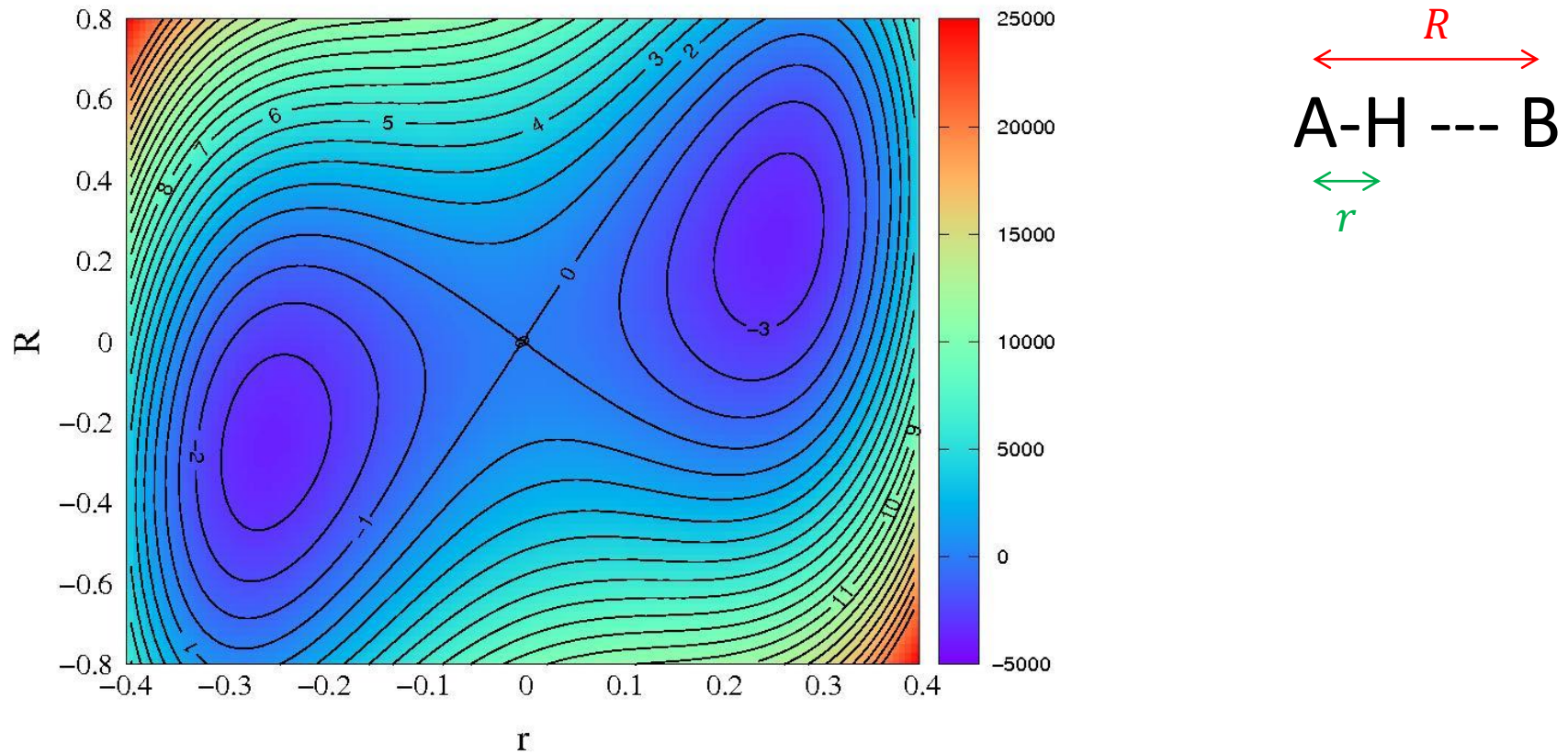


FIG. 1. Schematic illustration of the Azzouz–Borgis model for proton transfer between phenol (AH) and trimethylamine (B) in liquid methyl chloride. Adapted from Fig. 1 of Kim and Hammes-Schiffer (Ref. 2).

Proton Tunneling

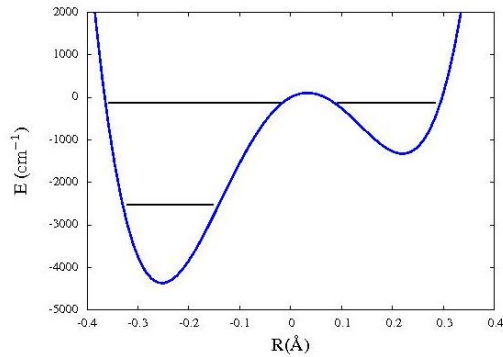


$$V_{cl}(R) = 0.5 M \omega^2 R^2$$

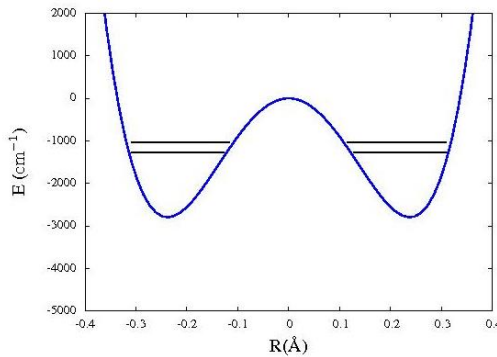
$$V_{QM}(r) = -0.5a_0 r^2 + 0.25c_0 r^4$$

$$V_{coup}(r, R) = -k \textcolor{blue}{r} \textcolor{red}{R}$$

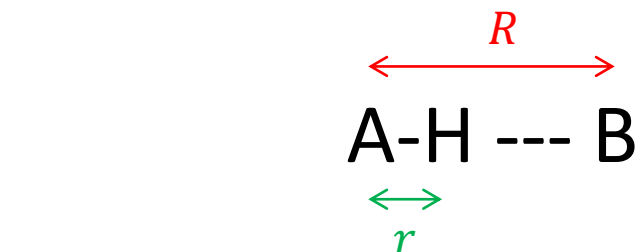
Proton Tunneling



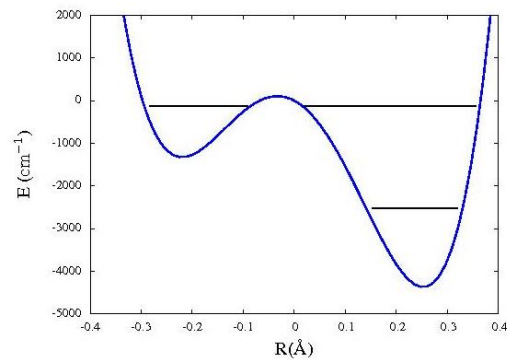
$$R = -0.22 \text{ \AA}$$



$$R = 0 \text{ \AA}$$



$$R = +0.22 \text{ \AA}$$



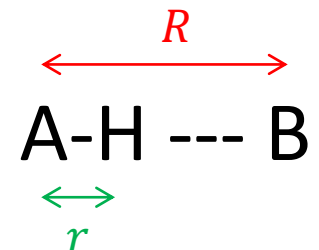
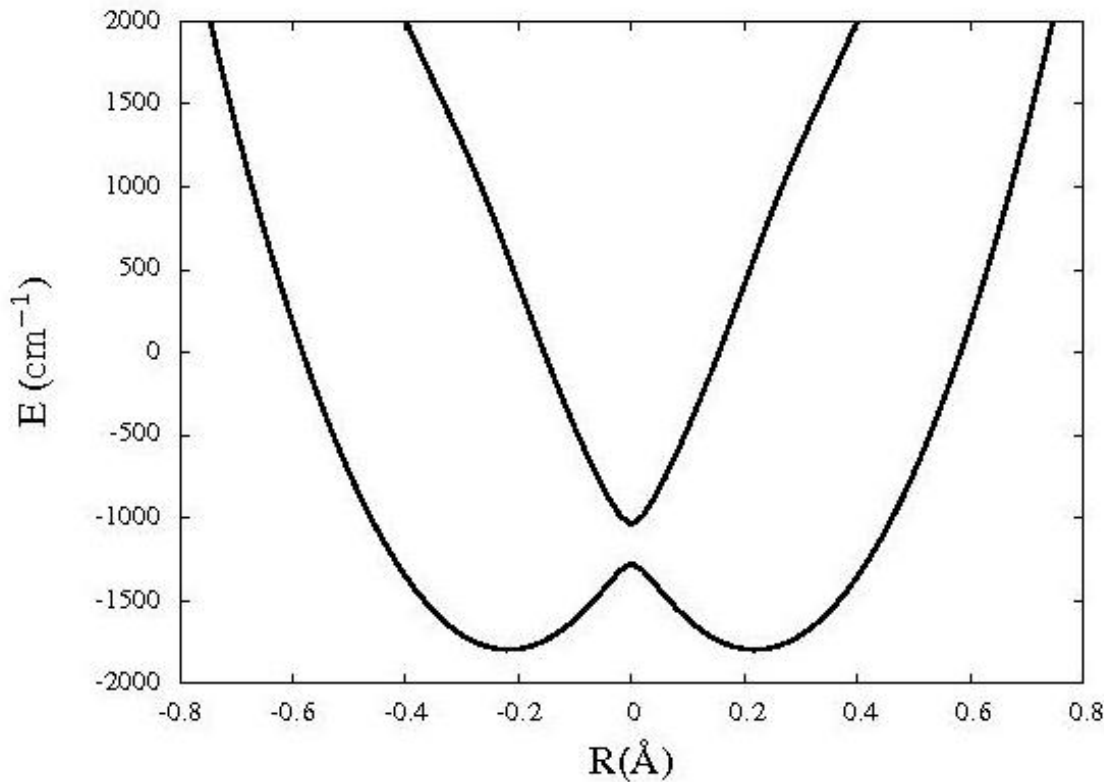
$$V_{cl}(R) = 0.5 M \omega^2 R^2$$

$$V_{QM}(r) = -0.5a_0 r^2 + 0.25c_0 r^4$$

$$V_{coup}(r, R) = -k \text{ } \color{blue}{r} \text{ } \color{red}{R}$$

Adiabatic Surfaces

General concepts: Hynes, Borgis



$$V_{cl}(R) = 0.5 M \omega^2 R^2$$

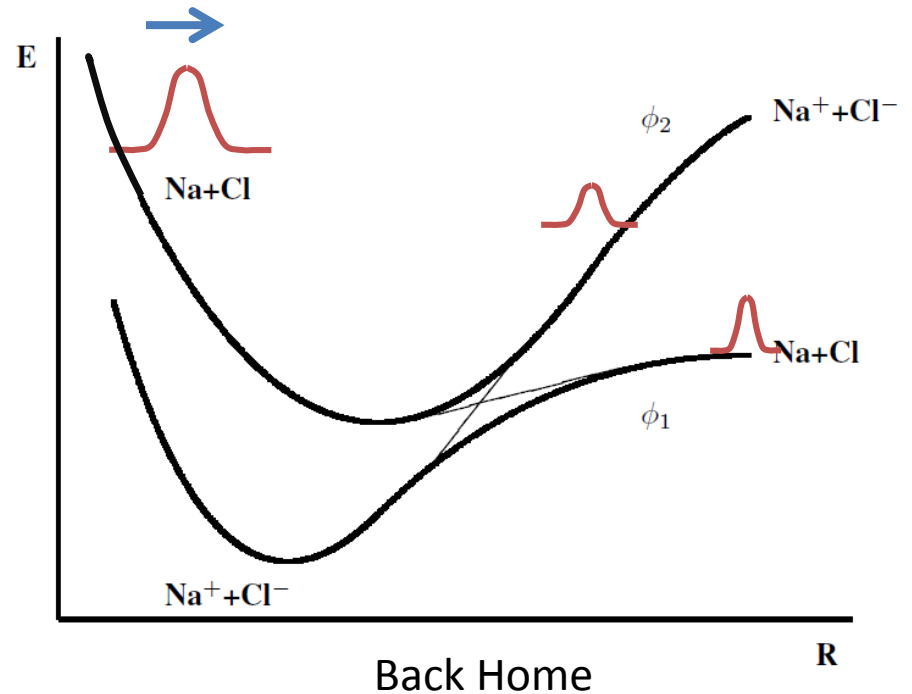
$$V_{QM}(r) = -0.5a_0r^2 + 0.25c_0r^4$$

$$V_{coup}(r, R) = -k \textcolor{blue}{r} \textcolor{red}{R}$$

Surface Hopping



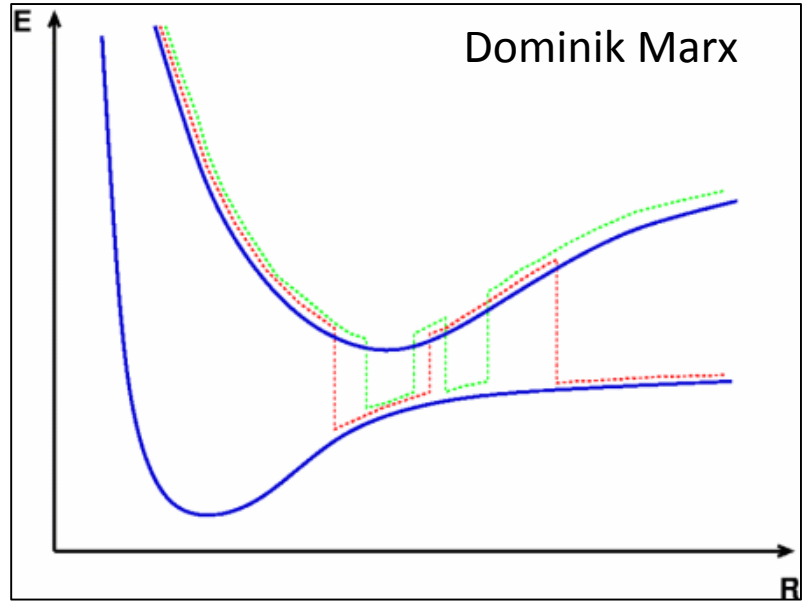
In Telluride



Surface Hopping



In Telluride



Back Home

Key Idea: Replace wave packets with classical trajectories.



ACS DIVISION OF PHYSICAL CHEMISTRY

243rd NATIONAL MEETING

San Diego, CA

March 25-29, 2012



NONADIABATIC DYNAMICS: SURFACE HOPPING AND BEYOND

Surface hopping, pioneered by Tully and Preston in 1971, represents the most popular family of non-adiabatic molecular dynamics (NAMD) techniques. NAMD has become a major approach for modeling chemical events that involve transitions between multiple quantum states. Surface hopping treats the transitions as stochastic events, in the spirit of the probabilistic interpretation of quantum mechanics. Examples of such studies abound, ranging from scattering of atoms and small molecules in gas phase, to photoinduced reactions in condensed phases, including solutions, polymers, inorganic materials and organic-inorganic interfaces, to biological processes such as photosynthesis and vision. The surface hopping simulations are strongly motivated by time-resolved optical experiments that are carried out by multiple research groups in every major research university. Some of the recent applications of NAMD include solar energy harvesting, inelastic processes in molecular electronics, biological optical probes, light emitting diodes, laser control of chemical reactivity and quantum information processing. The symposium aims for a timely discussion of modern developments, applications and challenges in surface hopping, nonadiabatic molecular dynamics and quantum dynamics in general.

Oleg Prezhdo, University of Rochester, prezhdo@chem.rochester.edu

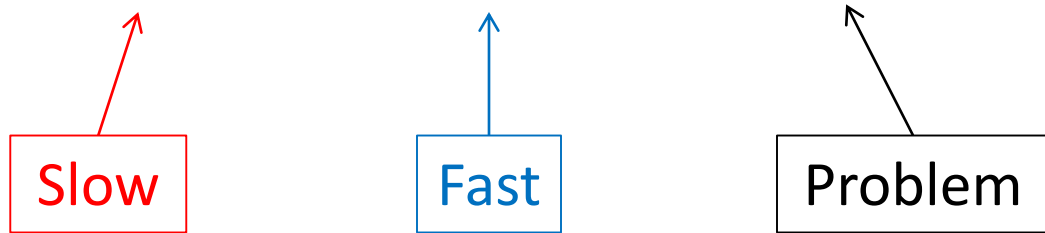
Xiaosong Li, University of Washington, li@chem.washington.edu

References

- http://www.theochem.ruhr-uni-bochum.de/~nikos.doltsinis/nic_10_doltsinis.pdf
- J. C. Tully, J. Chem. Phys. **93**, 1061 (1990)
- S. Hammes-Schiffer, J. Chem. Phys. **101**, 4657 (1994)
- J. Morelli, S. Hammes-Schiffer, Chem. Phys. Lett. **269**, 161 (1997)
- U. Muller, G. Stock, J. Chem. Phys. **107**, 6230 (1997)
- J. R. Schmidt, P. V. Parandekar, J. C. Tully, J. Chem. Phys. **129**, 44104 (2008)

Hamiltonian

$$H = H_{cl}(R) + H_{QM}(r) + V_{coup}(\mathbf{r}, R)$$



$$H_{cl}(R) = T_{cl} + V_{cl}(R)$$

$$H_{QM}(r) = T_{QM} + V_{QM}(r)$$

State of the system :

$$\mathbf{R}(t), \mathbf{P}(t), \psi_{QM}(\mathbf{r}, t)$$

Adiabatic Representation

$$H_{ad} = V_{cl}(R) + H_{QM} + V_{coup}(\textcolor{blue}{r}; \textcolor{red}{R})$$

$$H_{ad} \phi_i(\textcolor{blue}{r}; \textcolor{red}{R}) = E_i(\textcolor{red}{R}) \phi_i(\textcolor{blue}{r}; \textcolor{red}{R})$$

$E_i(\textcolor{red}{R})$ = Adiabatic Energy Surfaces
 $i = 0$: Born Oppenheimer approximation

Simple Approach

$$\dot{R} = P/m$$

$$\dot{P} = -\frac{\partial E_0(R)}{\partial R}$$

$$\psi_{QM}(r, t) = \phi_0(r; R(t)) e^{\frac{-iE_0(R)t}{\hbar}}$$

- Misses effect of excited energy surfaces.

Ehrenfest Dynamics

$$\dot{\mathbf{R}} = \mathbf{P}/m$$

$$\dot{\mathbf{P}} = -\frac{\partial <\psi|H_{ad}|\psi>_{\textcolor{blue}{r}}}{\partial \mathbf{R}}$$

$$\psi(\mathbf{r}, t) = \sum_j c_j(t) \phi_j(\textcolor{blue}{r}; \textcolor{red}{R}(t))$$

$$i\hbar \dot{c}_k = \sum_j c_j (V_{kj} - i\hbar \dot{\mathbf{R}} \cdot \mathbf{d}_{kj}) \quad V_{kj} = \int d\mathbf{r} \phi_k H_{ad} \phi_j = E_k \delta_{kj}$$
$$\mathbf{d}_{kj} = \int d\mathbf{r} \phi_k \nabla_{\textcolor{red}{R}} \phi_j$$

Mean field approximation

Limitation of E.D.

Mean Field Dynamics

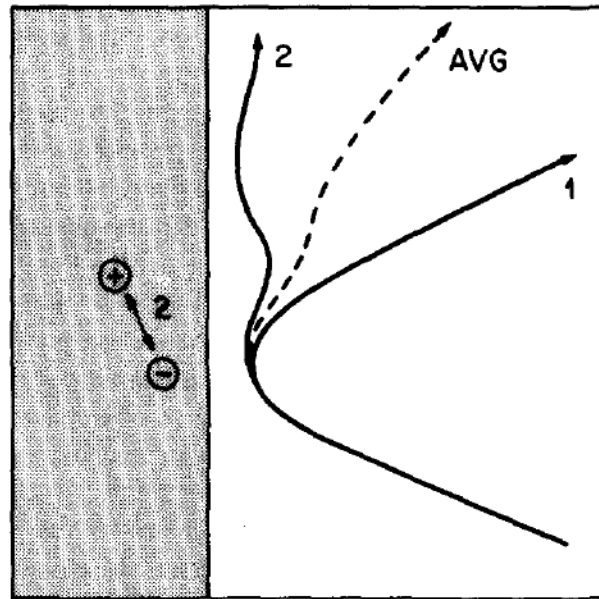


FIG. 1. Schematic illustration of a gas-surface scattering event showing two possible paths. If no electron-hole pair is excited in the solid (path 1), the gas scatters directly. If an electron-hole pair is excited (path 2), the loss of energy results in the gas remaining trapped on the surface. No average or best trajectory approach can adequately describe this situation.

Limitation of E.D.

Mean Field Dynamics

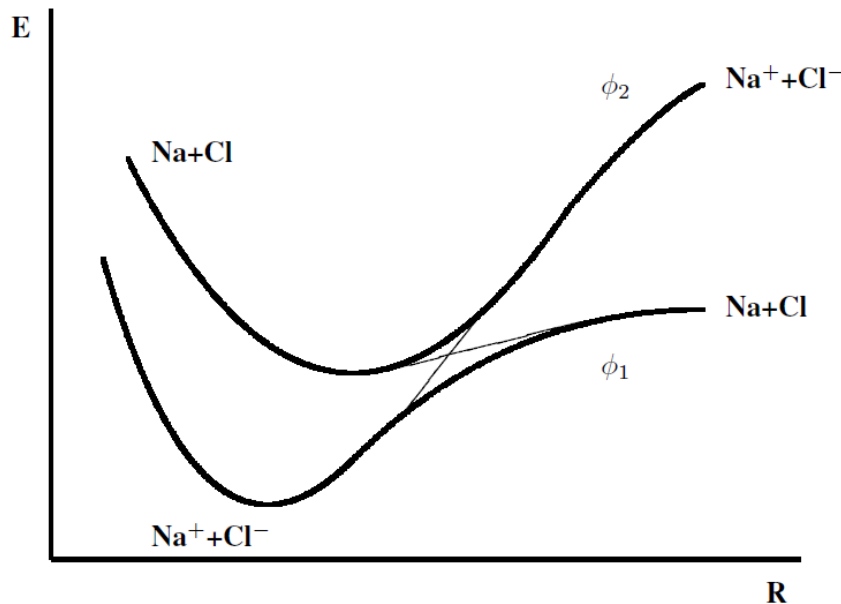


Figure 1. Avoided crossing between the covalent and ionic adiabatic potential curves of NaCl (thin lines: crossing of diabatic states).

Limitation of E.D.

No microreversibility

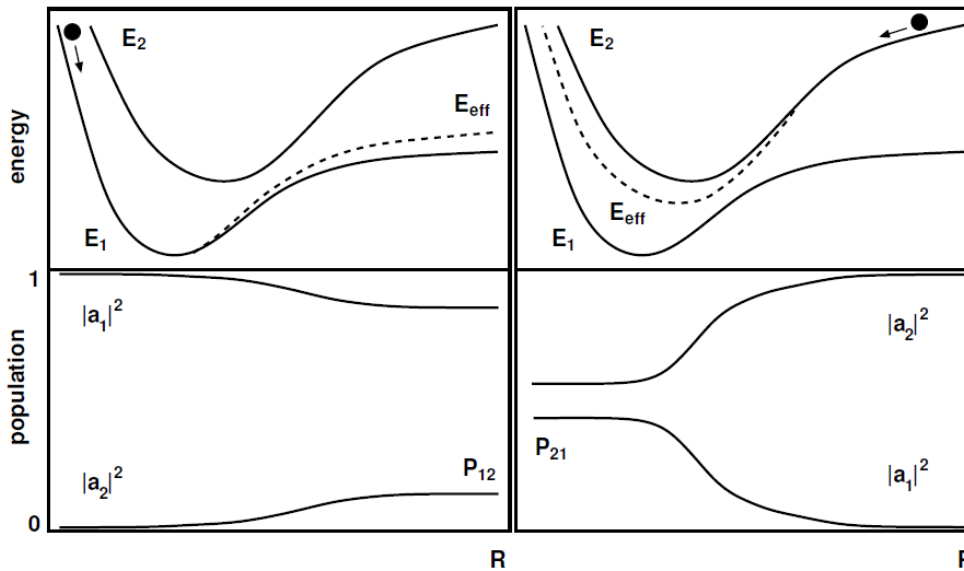
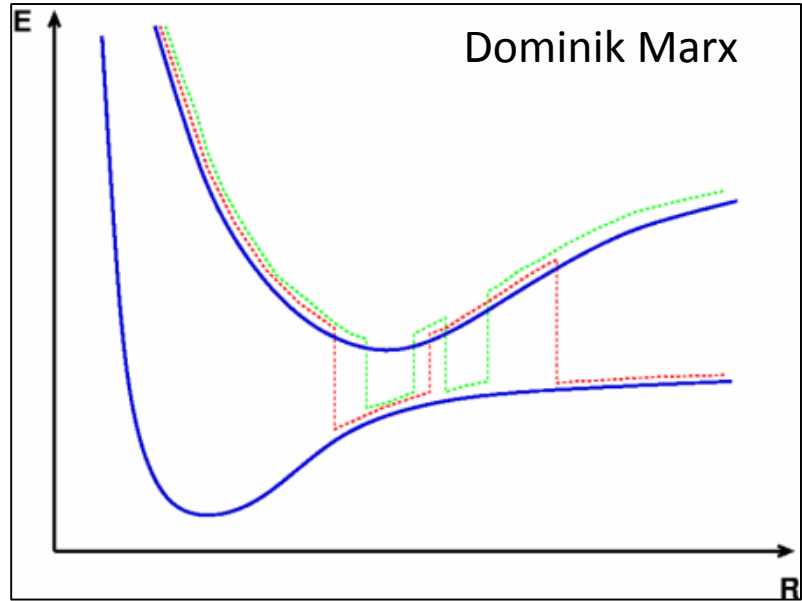


Figure 3. Top left: forward path effective potential, E_{eff} , for two weakly coupled adiabatic PES, E_1 and E_2 . Bottom left: state occupations for a system initially prepared in state 1. The final value of $|a_2|^2$ is equal to the transition probability P_{12} . Top right: backward path effective potential, E_{eff} , for two weakly coupled adiabatic PES, E_1 and E_2 . Bottom left: state occupations for a system initially prepared in state 2. The final value of $|a_1|^2$ is equal to the transition probability P_{21} .

Surface Hopping



In Telluride



Back Home

Key Idea: Replace wave packets with classical trajectories.

Surface Hopping

$$\dot{\mathbf{R}} = \mathbf{P}/m$$

$$\dot{\mathbf{P}} = -\frac{\partial E_k(\mathbf{R})}{\partial \mathbf{R}}$$

$$\psi(r, t) = \sum_j c_j(t) \phi_j(\mathbf{r}; \mathbf{R}(t))$$

$$i\hbar \dot{c}_k = \sum_j c_j (V_{kj} - i\hbar \dot{\mathbf{R}} \cdot \mathbf{d}_{kj}) \quad V_{kj} = \int dr \phi_k H_{ad} \phi_j = E_k \delta_{kj}$$
$$\mathbf{d}_{kj} = \int dr \phi_k \nabla_{\mathbf{R}} \phi_j$$

Trajectories hopping to/from state k, s.t.

$$\dot{N}_k = |c_k|^2 *$$

* Approximately true due to frustrated hops

Hopping Mechanism

Defining $a_{kj} = c_k c_j^*$

$$\dot{a}_{kk} = \sum_{k' \neq k} b_{kk'}$$

$$b_{kk'} = 2\hbar^{-1} \text{Im}(a_{kk'}^* V_{kk'}) - 2\text{Re}(a_{kk'}^* \mathbf{R} \cdot \mathbf{d}_{kk'})$$

At time t, fraction of trajectories in state $k = a_{kk}$

At time $t+dt$, fraction of trajectories in state $k = a_{kk} + \dot{a}_{kk} dt$

Probability of 'hopping' from state $k = -\frac{\dot{a}_{kk} dt}{a_{kk}} = \frac{\sum_{k' \neq k} b_{k'k} dt}{a_{kk}}$

Probability of 'hopping' from state k to state $k' = \frac{b_{k'k} dt}{a_{kk}}$

Hopping Mechanism

Rate of ‘hopping’ from state k to state k' =

$$\frac{(a_{kk'}^* + a_{kk'})}{a_{kk}} \dot{\mathbf{R}} \cdot \mathbf{d}_{kk'}$$

- Rate $\propto a_{kk'}$
- Rate $\propto \dot{\mathbf{R}}$
- Rate $\propto \mathbf{d}_{kk'}$

Energy Conservation

Direction of Force during hop = $\mathbf{d}_{kk'}$
 $[<\phi_k|\nabla_{\textcolor{red}{R}} H|\phi_{k'}>_r = -(E_{k'} - E_k)\mathbf{d}_{k'k}]$

$$\mathbf{P}' = \mathbf{P} - \gamma_{k'k}\mathbf{d}_{k'k}, \text{ s.t.}$$

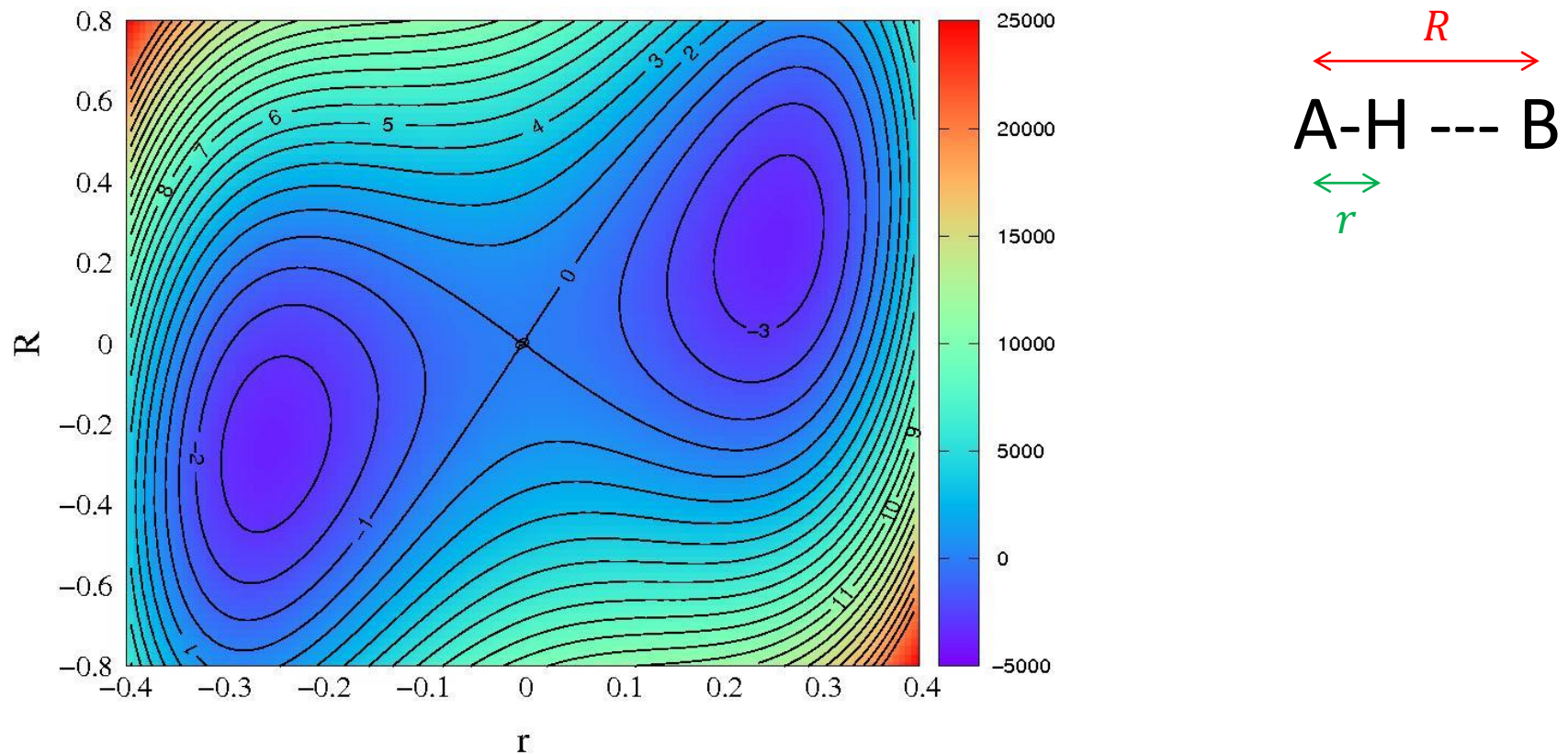
$$\sum_i \frac{{P'_i}^2}{2m_i} + E_{k'} = \sum_i \frac{{P_i}^2}{2m_i} + E_k$$

If γ complex, frustrated hop (no hop takes place)

Limitations of S.H.

- Artificial coherence
- Discontinuous change of velocity during hop
- All nuclear d.o.f. treated same during hop (γ independent of nuclei)
- Frustrated hops
- Multiple hops

Proton Tunneling

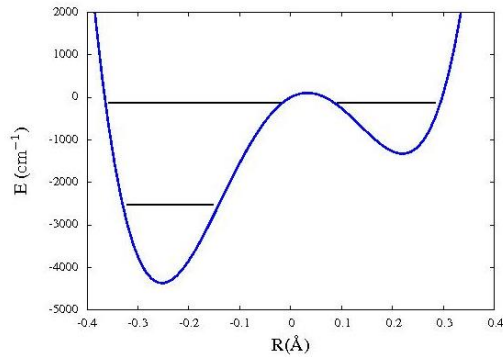


$$V_{cl}(R) = 0.5 M \omega^2 R^2$$

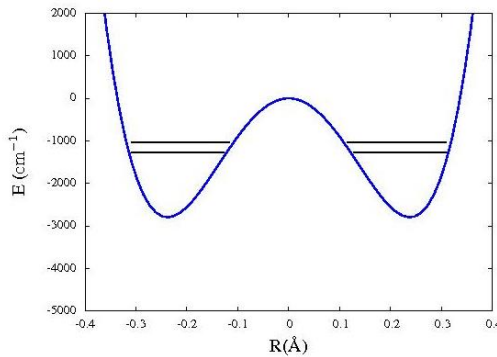
$$V_{QM}(r) = -0.5a_0 r^2 + 0.25c_0 r^4$$

$$V_{coup}(r, R) = -k \textcolor{blue}{r} \textcolor{red}{R}$$

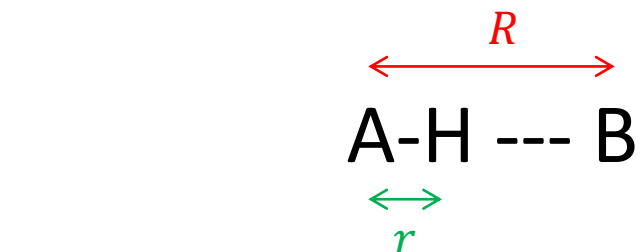
Proton Tunneling



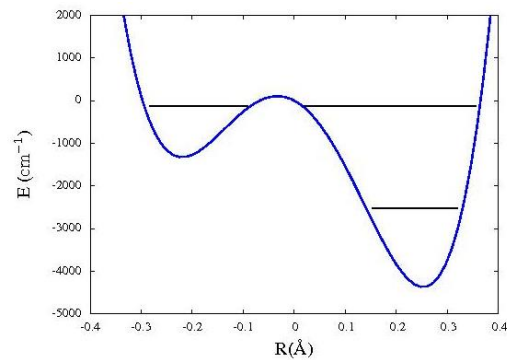
$$R = -0.22 \text{ \AA}$$



$$R = 0 \text{ \AA}$$



$$R = +0.22 \text{ \AA}$$

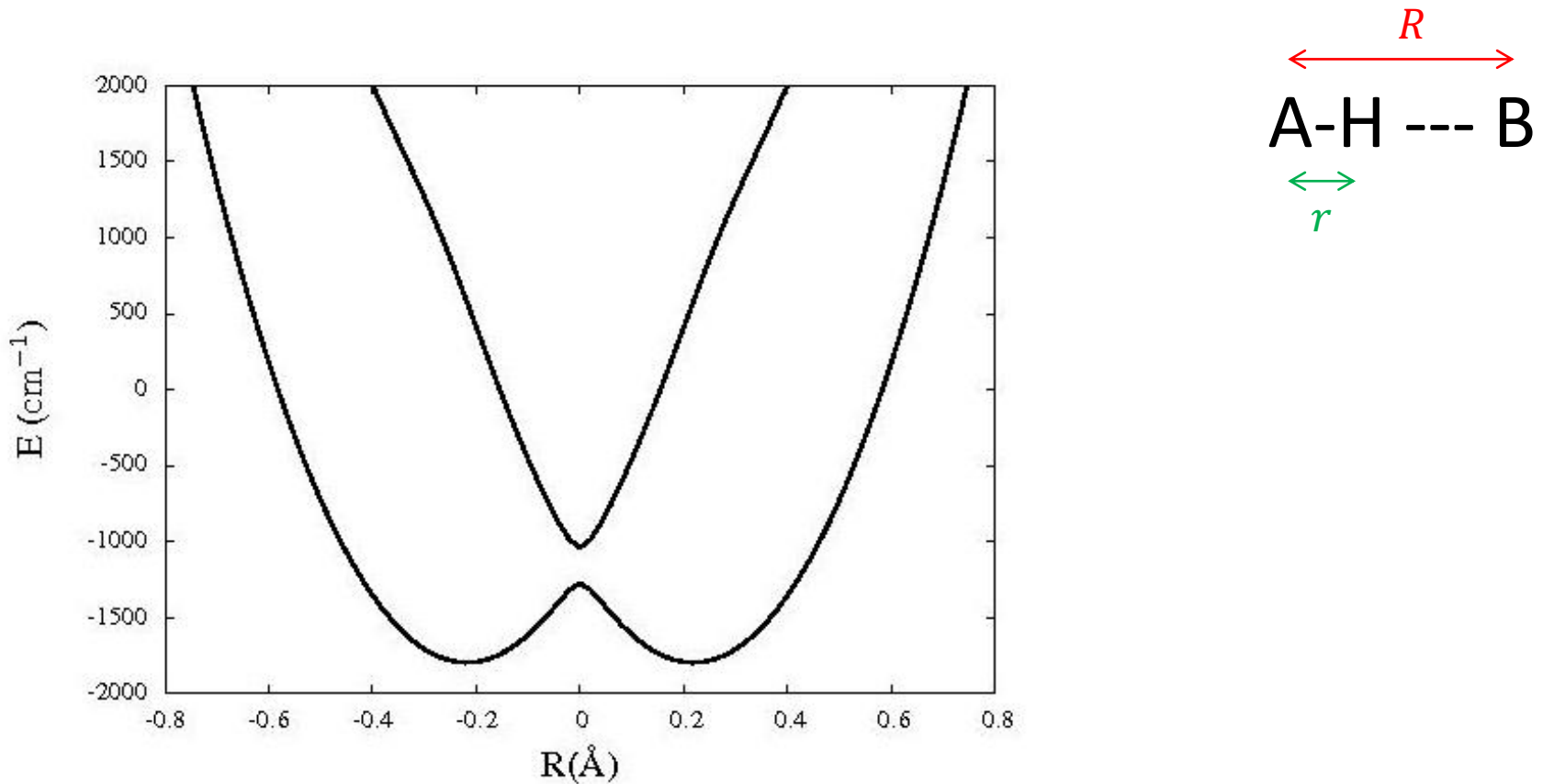


$$V_{cl}(R) = 0.5 M \omega^2 R^2$$

$$V_{QM}(r) = -0.5a_0r^2 + 0.25c_0r^4$$

$$V_{coup}(r, R) = -k \text{ } \color{blue}{r} \text{ } \color{red}{R}$$

Adiabatic Surfaces

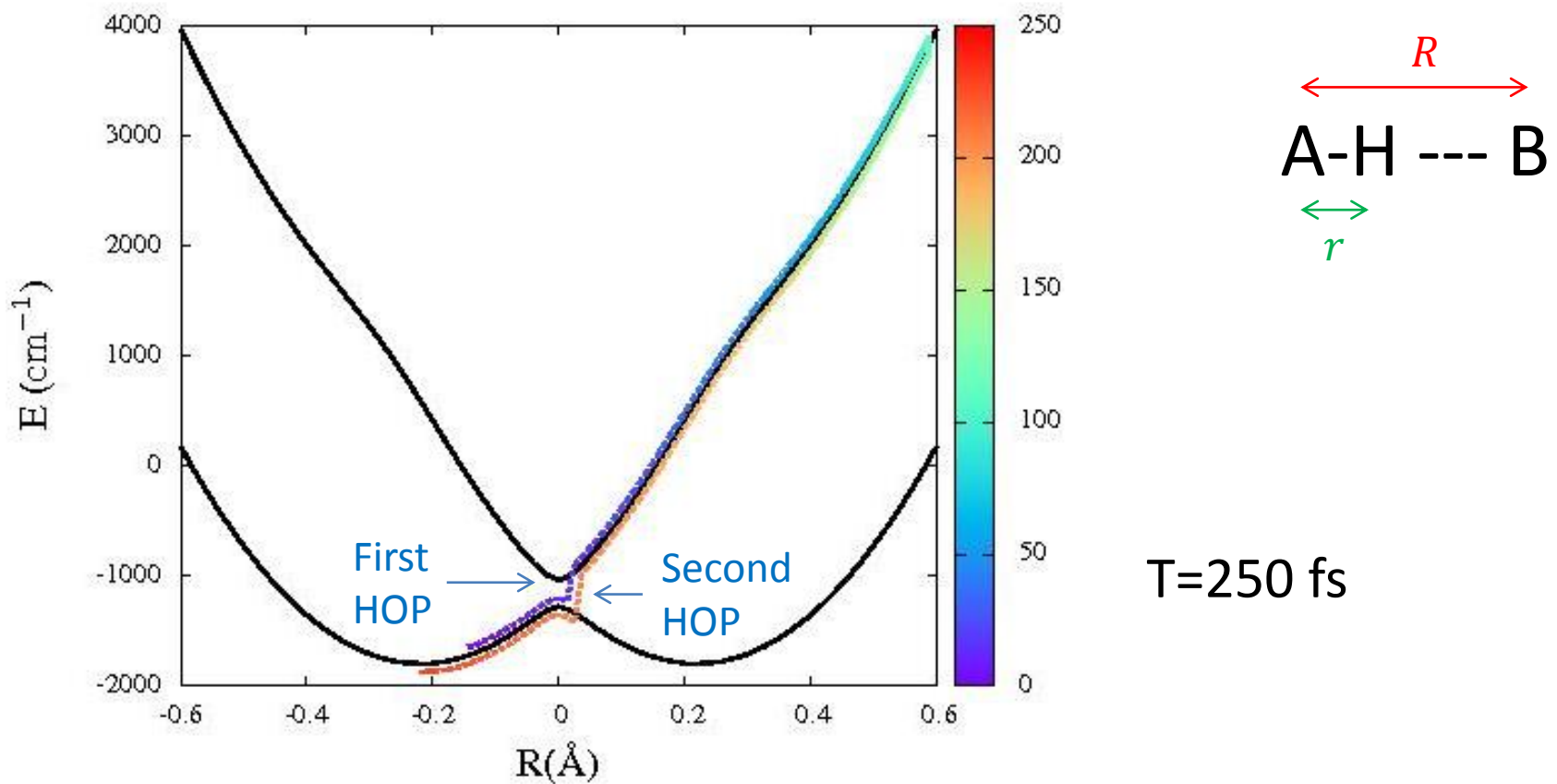


$$V_{cl}(R) = 0.5 M \omega^2 R^2$$

$$V_{QM}(r) = -0.5a_0r^2 + 0.25c_0r^4$$

$$V_{coup}(r, R) = -k \textcolor{blue}{r} \textcolor{red}{R}$$

Trajectory

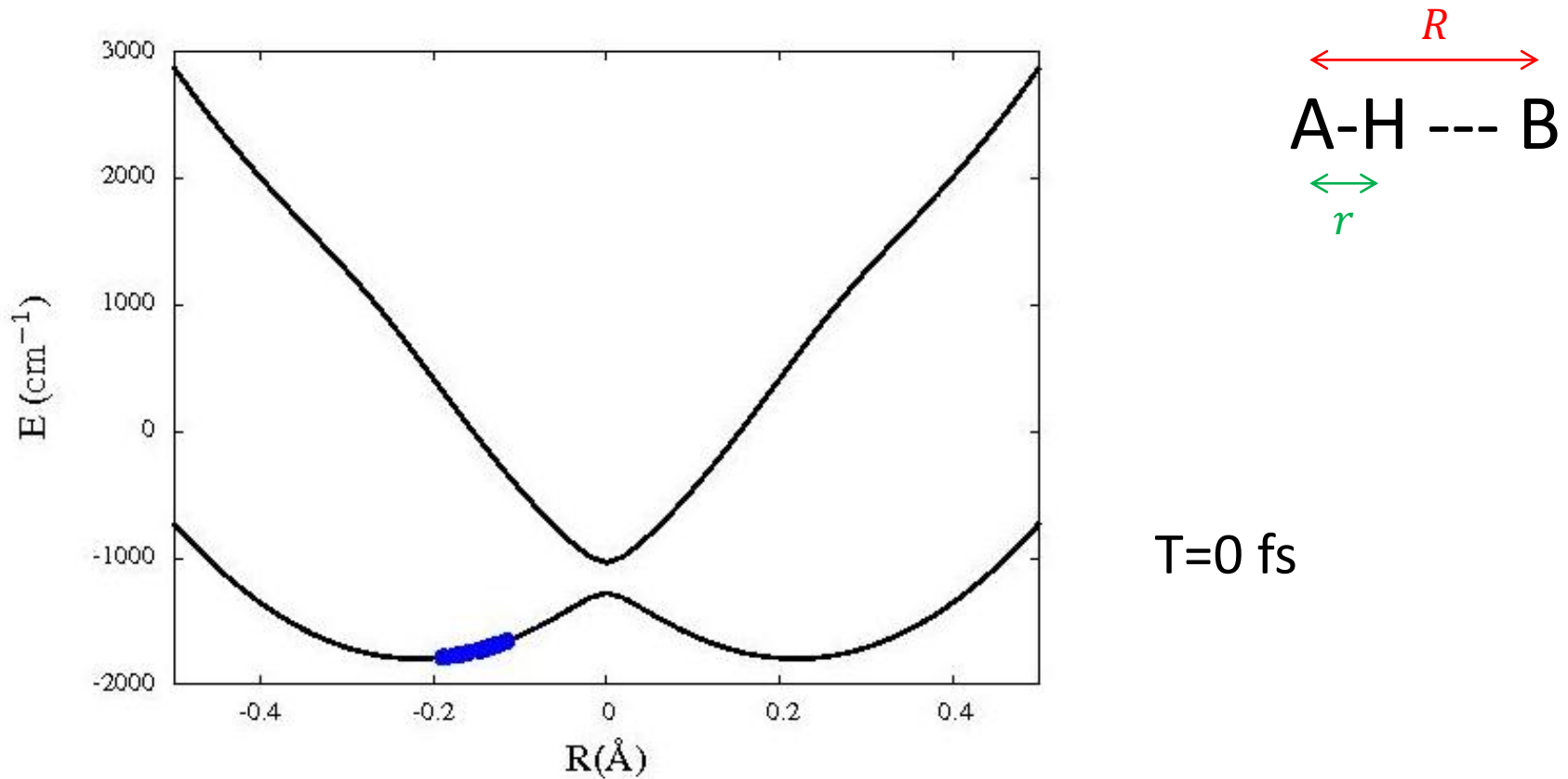


$$V_{cl}(R) = 0.5 M \omega^2 R^2$$

$$V_{QM}(r) = -0.5a_0 r^2 + 0.25c_0 r^4$$

$$V_{coup}(r, R) = -k \textcolor{blue}{r} \textcolor{red}{R}$$

Trajectory

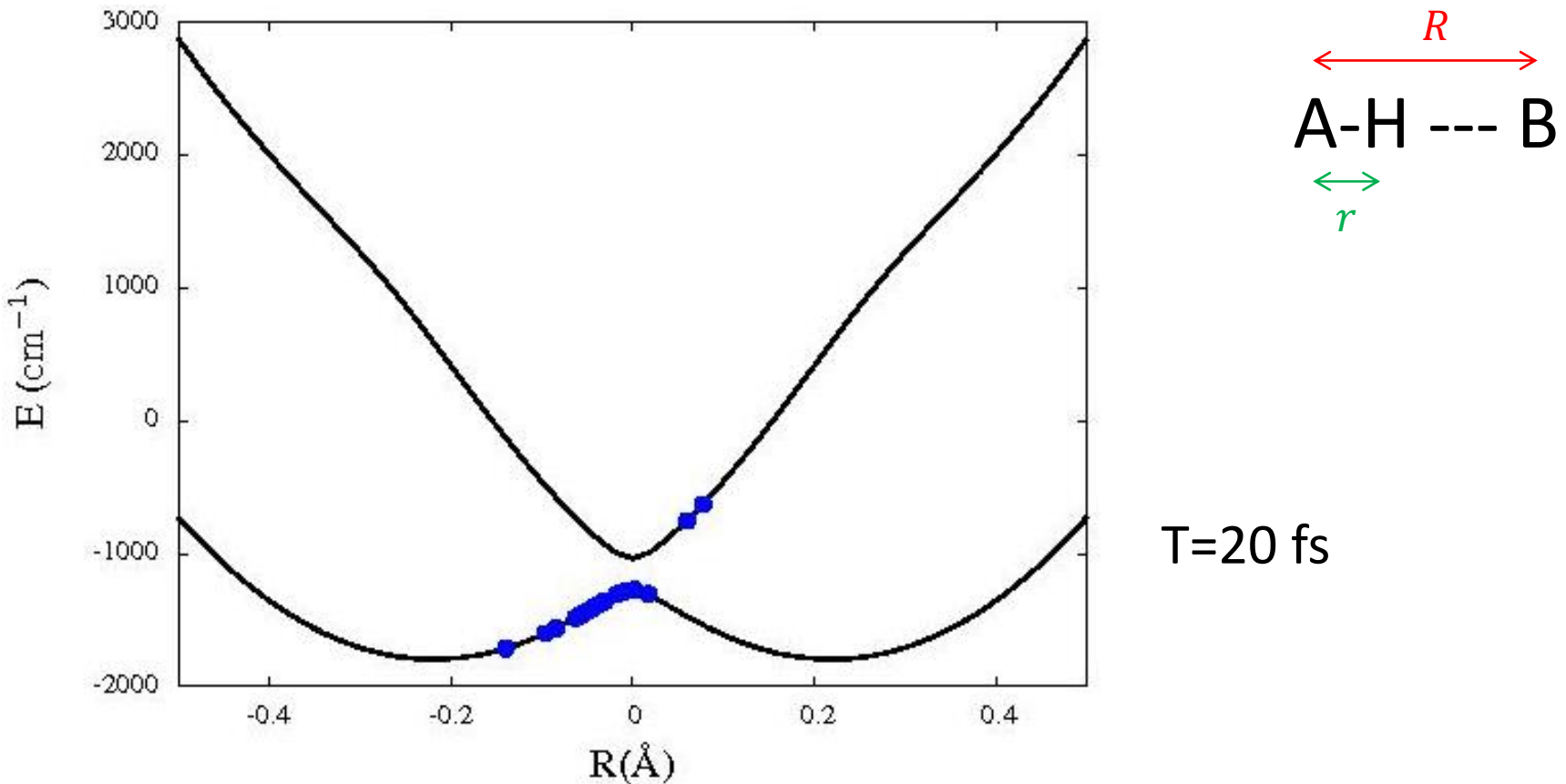


$$V_{cl}(R) = 0.5 M \omega^2 R^2$$

$$V_{QM}(r) = -0.5a_0r^2 + 0.25c_0r^4$$

$$V_{coup}(r, R) = -k \textcolor{blue}{r} \textcolor{red}{R}$$

Trajectory



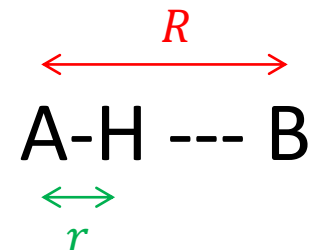
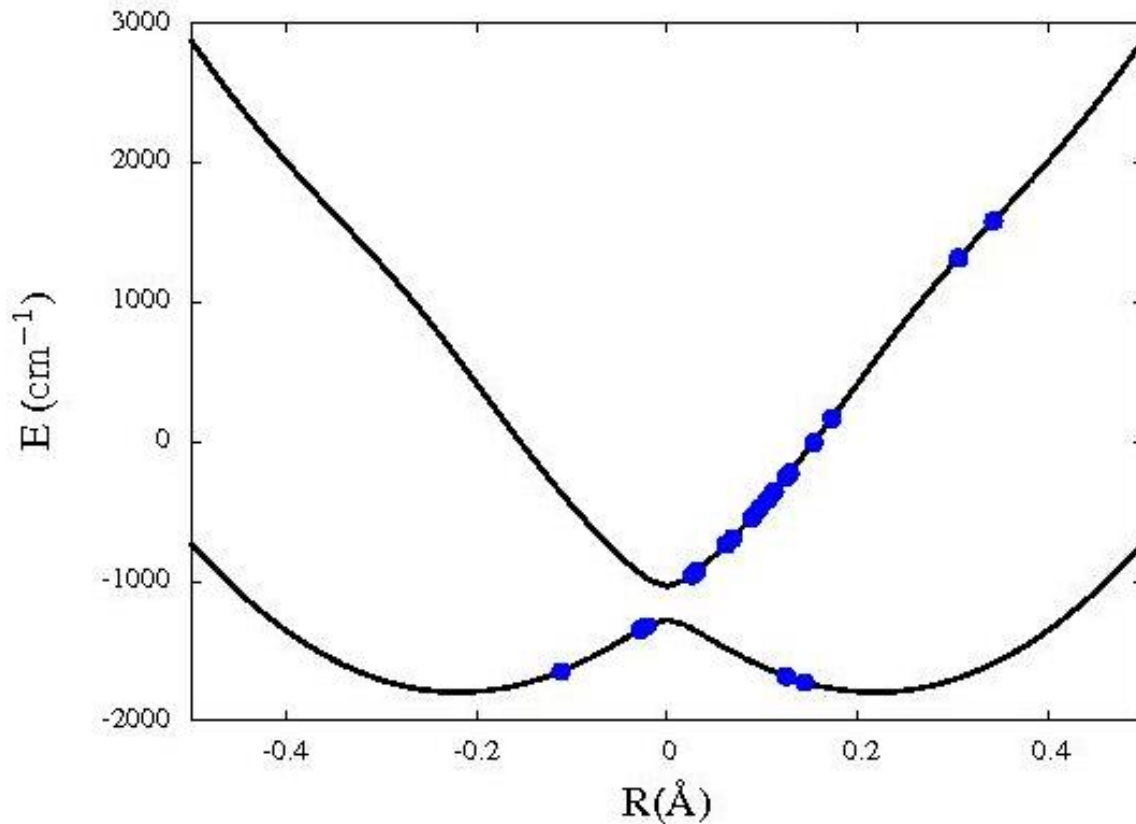
$T=20 \text{ fs}$

$$V_{cl}(R) = 0.5 M \omega^2 R^2$$

$$V_{QM}(r) = -0.5a_0r^2 + 0.25c_0r^4$$

$$V_{coup}(r, R) = -k \textcolor{blue}{r} \textcolor{red}{R}$$

Trajectory



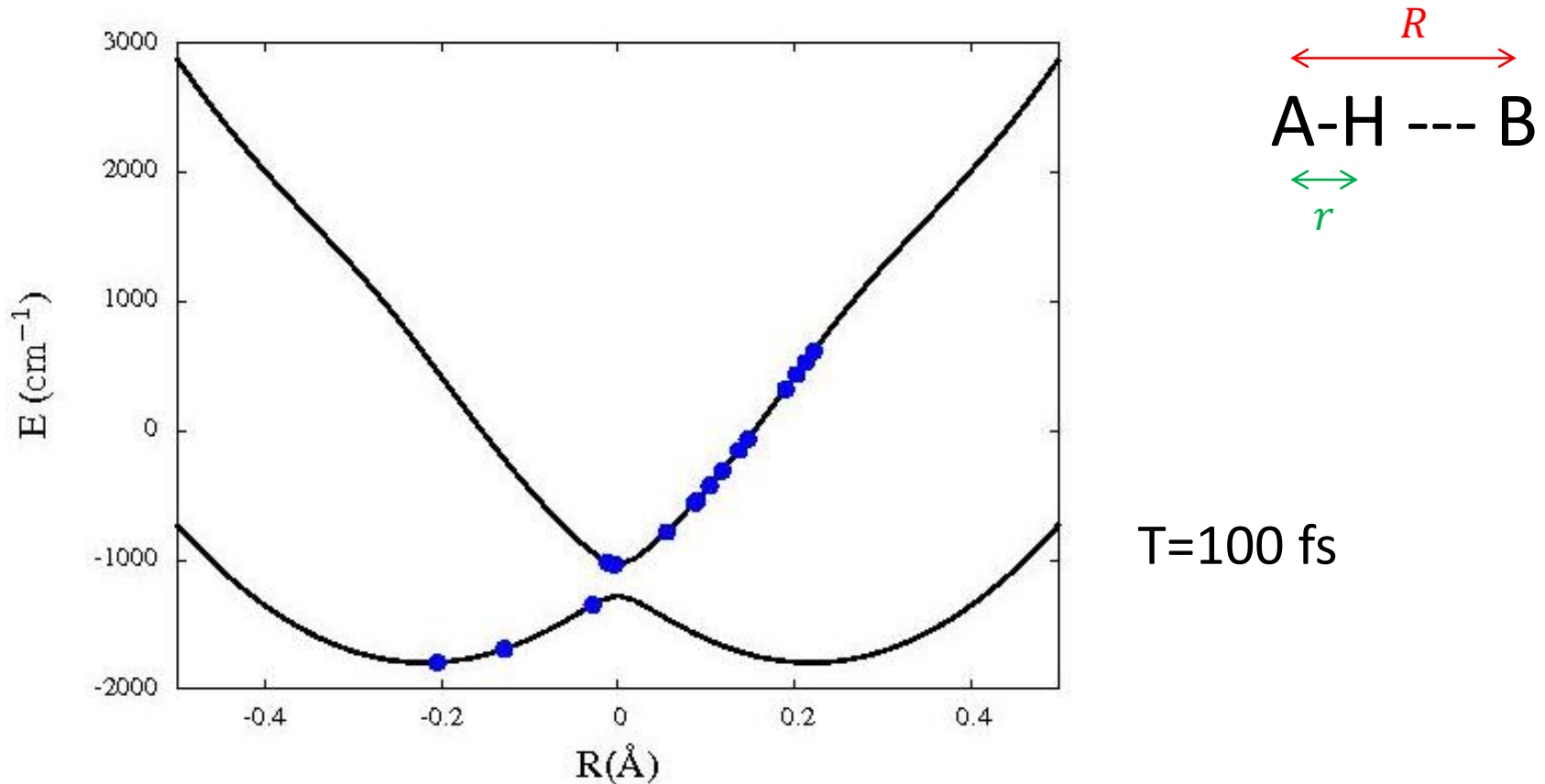
$T=50$ fs

$$V_{cl}(R) = 0.5 M \omega^2 R^2$$

$$V_{QM}(r) = -0.5a_0 r^2 + 0.25c_0 r^4$$

$$V_{coup}(r, R) = -k \textcolor{blue}{r} \textcolor{red}{R}$$

Trajectory

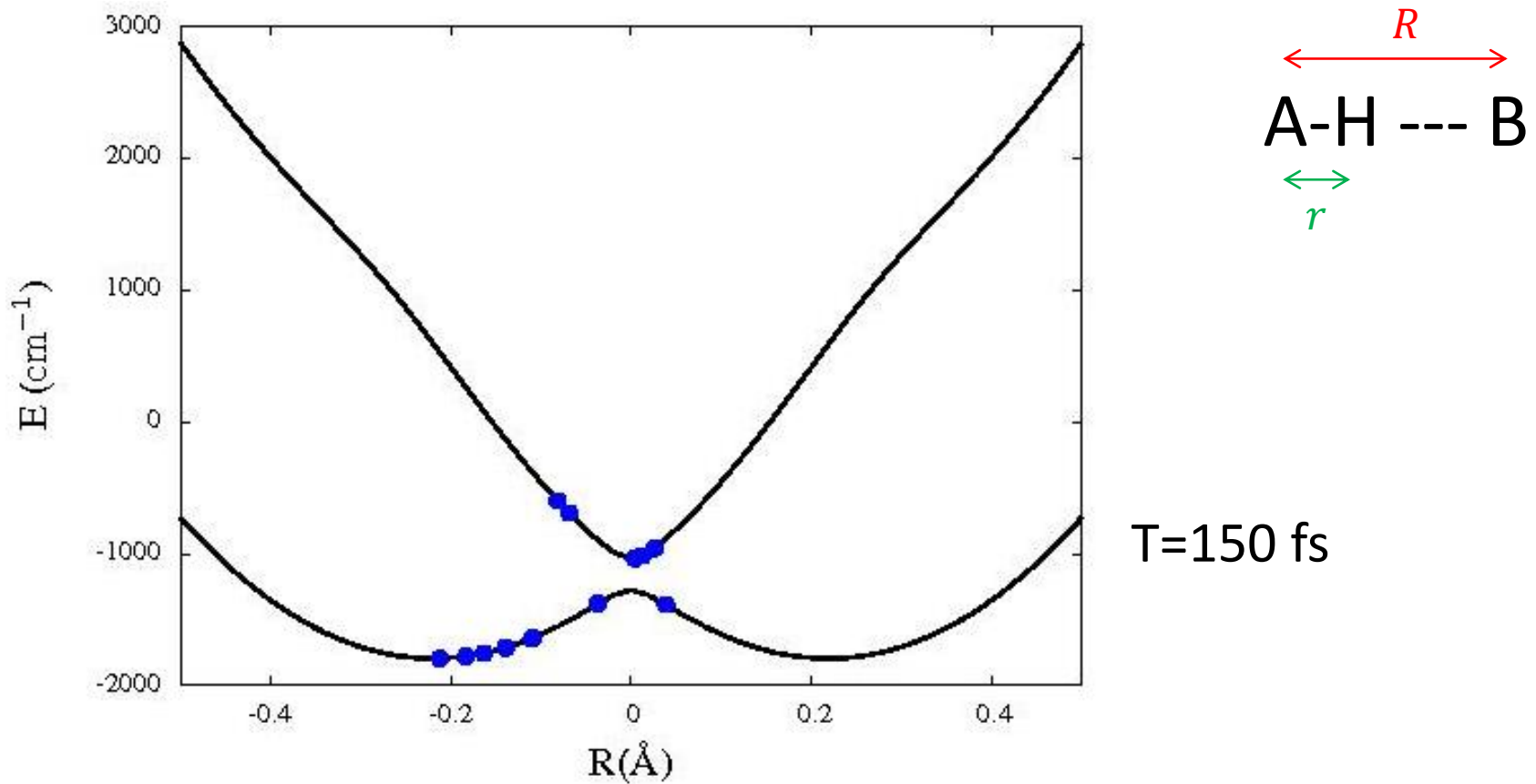


$$V_{cl}(R) = 0.5 M \omega^2 R^2$$

$$V_{QM}(r) = -0.5a_0r^2 + 0.25c_0r^4$$

$$V_{coup}(r, R) = -k \textcolor{blue}{r} \textcolor{red}{R}$$

Trajectory

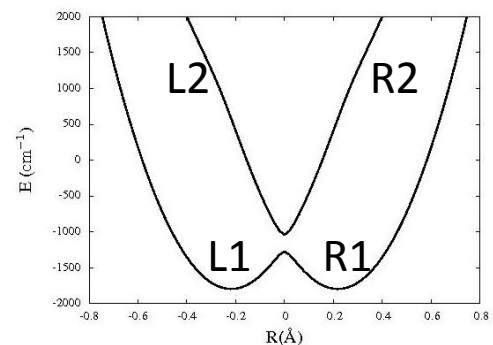
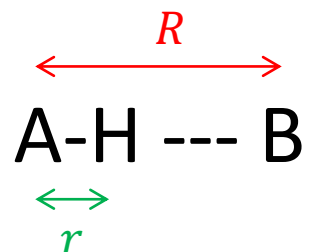
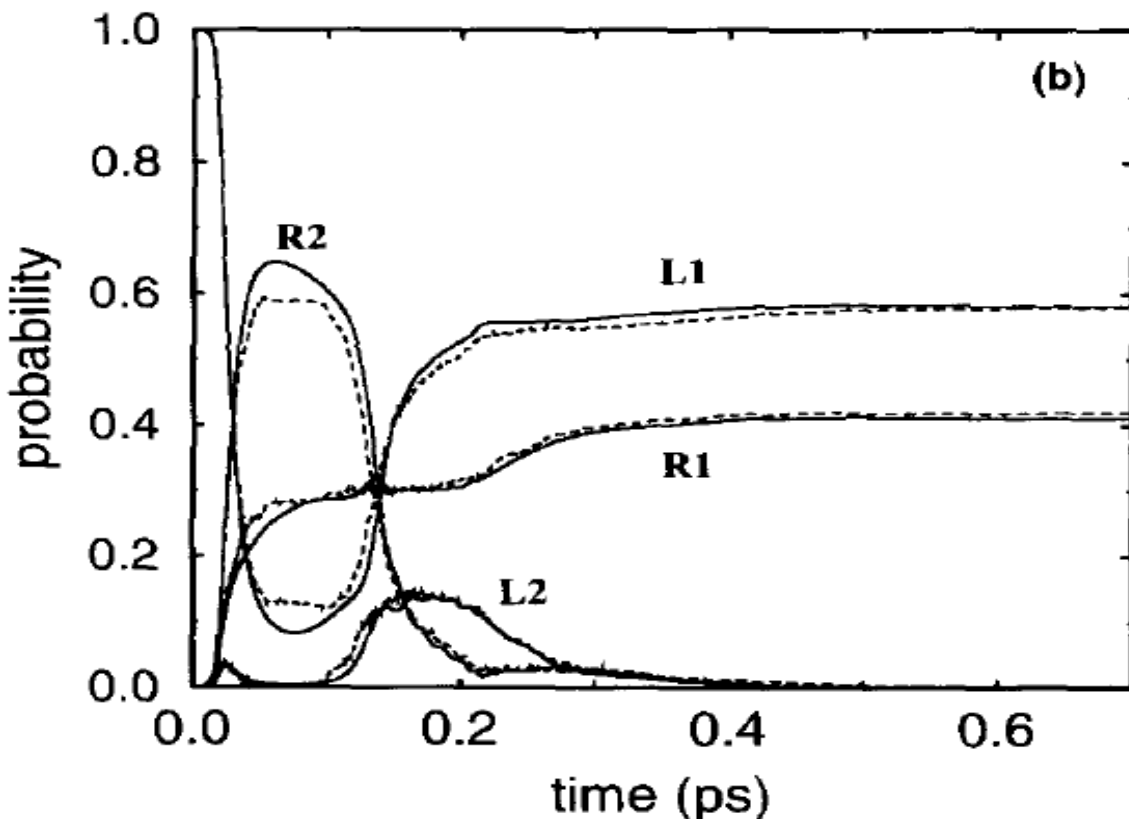


$$V_{cl}(R) = 0.5 M \omega^2 R^2$$

$$V_{QM}(r) = -0.5a_0r^2 + 0.25c_0r^4$$

$$V_{coup}(r, R) = -k \textcolor{blue}{r} \textcolor{red}{R}$$

Comparison to full Q.M.



$$V_{cl}(R) = 0.5 M \omega^2 R^2$$

$$V_{QM}(r) = -0.5a_0r^2 + 0.25c_0r^4$$

$$V_{coup}(r, R) = -k \textcolor{blue}{r} \textcolor{red}{R}$$

Alternatives to S.H.

- Instanton Trajectory
 - J. P. Sethna, Phys. Rev. B **24**, 698 (1981)
- Initial Value Representation
 - W. H. Miller, J. Phys. Chem. A. **105**, 2942 (2001)
- Ring Polymer Molecular Dynamics
 - I. R. Craig, D. E. Manolopoulos, J. Chem. Phys. **121**, 3368 (2004)
- Semiclassical Tunneling
 - N. Makri, W. H. Miller, J. Chem. Phys. **91**, 4026 (1989)
- Ab Initio Multiple Spawning
 - M. Ben-Nun, T. Martinez, J. Chem. Phys. **108**, 7244 (1998)

TDSCF

$$\frac{i}{\hbar} \partial_t \Psi = H \Psi$$

$$\Psi = \chi(x) \psi(y) e^{i\gamma(t)/\hbar} \equiv \chi \psi e^{i\gamma/\hbar}$$

$$\frac{i}{\hbar} \partial_t \chi \psi e^{i\gamma/\hbar} = H \chi \psi e^{i\gamma/\hbar}$$

TDSCF

$$\frac{i}{\hbar} \partial_t \chi \psi e^{i\gamma/\hbar} = H \chi \psi e^{i\gamma/\hbar}$$

$$\frac{i}{\hbar} \left[[\partial_t \chi] \psi + \chi [\partial_t \psi] \right] - \chi \psi \dot{\gamma} = H \chi \psi$$

$$\frac{i}{\hbar} \left[\partial_t \chi + \langle \psi | \partial_t \psi \rangle \chi \right] - \chi \dot{\gamma} = \langle \psi | H | \psi \rangle \chi$$

$$\frac{i}{\hbar} \left[\partial_t \psi + \langle \chi | \partial_t \chi \rangle \psi \right] - \psi \dot{\gamma} = \langle \chi | H | \chi \rangle \psi$$

TDSCF

$$\frac{i}{\hbar} [\partial_t \chi + \langle \psi | \partial_t \psi \rangle \chi] - \chi \dot{\gamma} = \langle \psi | H | \psi \rangle \chi$$

$$\frac{i}{\hbar} [\partial_t \psi + \langle \chi | \partial_t \chi \rangle \psi] - \psi \dot{\gamma} = \langle \chi | H | \chi \rangle \psi$$

Set $\dot{\gamma} = \frac{i}{\hbar} \langle \psi | \partial_t \psi \rangle = \frac{i}{\hbar} \langle \chi | \partial_t \chi \rangle$

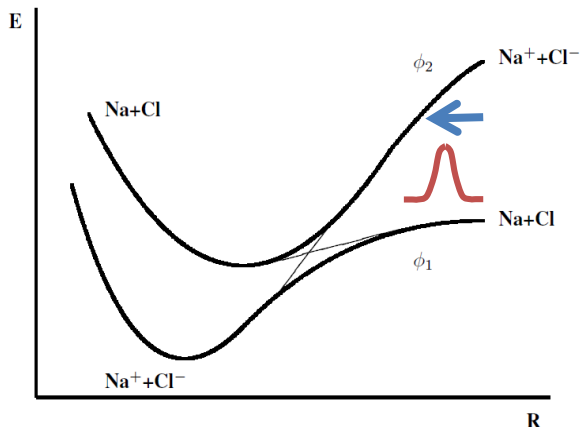
$$\frac{i}{\hbar} \partial_t \chi = \langle \psi | H | \psi \rangle \chi$$

$$\frac{i}{\hbar} \partial_t \psi = \langle \chi | H | \chi \rangle \psi$$

Using these equations solve for $\dot{\gamma}$

TDSCF

$$\Psi = \chi \psi$$



MCTDSCF

$$\Psi = \begin{pmatrix} \chi_1 \psi_1 \\ \chi_2 \psi_2 \end{pmatrix}$$

Rows correspond to different electronic states. The χ_i and ψ_i correspond to the system and bath in this example

Think Pair Share

There are several possibilities for the normalizing
 $\Psi = \chi_1\psi_1 + \chi_2\psi_2$. Which one do you prefer?

- a) $\langle \chi_1 | \chi_1 \rangle = \langle \chi_2 | \chi_2 \rangle = 1; \quad \langle \psi_1 | \psi_1 \rangle = \langle \psi_2 | \psi_2 \rangle = 1$
- b) $\langle \chi_1 | \chi_1 \rangle + \langle \chi_2 | \chi_2 \rangle = 1; \quad \langle \psi_1 | \psi_1 \rangle = \langle \psi_2 | \psi_2 \rangle = 1$
- c) $\langle \chi_1 | \chi_1 \rangle = \langle \chi_2 | \chi_2 \rangle = 1; \quad \langle \psi_1 | \psi_1 \rangle + \langle \psi_2 | \psi_2 \rangle = 1$
- d) $\langle \chi_1 | \chi_1 \rangle + \langle \chi_2 | \chi_2 \rangle = 1; \quad \langle \psi_1 | \psi_1 \rangle + \langle \psi_2 | \psi_2 \rangle = 1$

TDSCF

MCTDSCF

$$\frac{i}{\hbar} \partial_t \Psi = H\Psi$$



$$\Psi = \begin{pmatrix} \chi_1 \psi_1 \\ \chi_2 \psi_2 \end{pmatrix}$$

$$\frac{i}{\hbar} \partial_t \chi \psi = H \chi \psi \rightarrow \frac{i}{\hbar} \partial_t \begin{pmatrix} \chi_1 \psi_1 \\ \chi_2 \psi_2 \end{pmatrix} = \begin{pmatrix} H_{11} & H_{12} \\ H_{21} & H_{22} \end{pmatrix} \begin{pmatrix} \chi_1 \psi_1 \\ \chi_2 \psi_2 \end{pmatrix}$$

$$\frac{i}{\hbar} \partial_t \psi = \langle \chi | H | \chi \rangle \psi \rightarrow \frac{i}{\hbar} \partial_t \chi_1 = \langle \psi_1 | H_{11} | \psi_1 \rangle \chi_1 + \langle \psi_2 | H_{12} | \psi_1 \rangle \chi_2$$
$$\frac{i}{\hbar} \partial_t \chi_2 = \langle \psi_1 | H_{21} | \psi_2 \rangle \chi_1 + \langle \psi_2 | H_{22} | \psi_2 \rangle \chi_2$$

Validity of time-dependent self-consistent-field (TDSCF) approximations for unimolecular dynamics: A test for photodissociation of the Xe–HI cluster

R. Alimi

*Department of Physical Chemistry and The Fritz Haber Center for Molecular Dynamics,
The Hebrew University of Jerusalem, Jerusalem 91904, Israel*

R. B. Gerber

*Department of Physical Chemistry and The Fritz Haber Center for Molecular Dynamics,
The Hebrew University of Jerusalem, Jerusalem 91904, Israel and Department of Chemistry,
University of California, Irvine, California 92717*

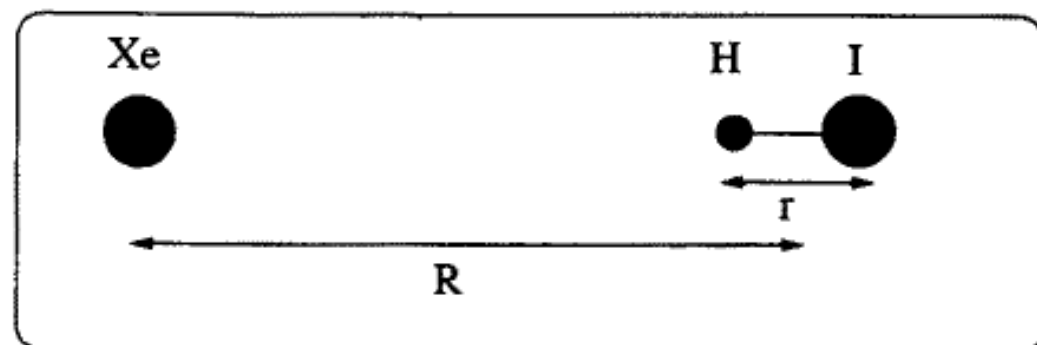
A. D. Hammerich and R. Kosloff

*Department of Physical Chemistry and The Fritz Haber Center for Molecular Dynamics,
The Hebrew University of Jerusalem, Jerusalem 91904, Israel*

M. A. Ratner

Department of Chemistry, Northwestern University, Evanston, Illinois 60208

(Received 18 December 1989; accepted 11 July 1990)



$$V(r,R) \approx V_{\text{H-I}}(r) + V_{\text{H-Xe}}(R-r) + V_{\text{Xe-I}}(R).$$

FIG. 1. Coordinate system for the collinear model Xe–HI.

Time-dependent Hartree approaches for the study of intramolecular dynamics in dimer systems

Pierre-Nicholas Roy^{a)}

Department of Chemistry, University of Alberta, Edmonton, Alberta T6G 2G2, Canada

John C. Light

The James Franck Institute, The University of Chicago, Chicago, Illinois 60637

(Received 29 November 1999; accepted 29 March 2000)

We apply and the time-dependent Hartree (TDH) method to the study of intramolecular dynamics in dimer systems. The HCl dimer is chosen as test case. Model calculations are performed on reduced dimensional representation of this system namely two-, three-, and four-dimensional ones. We assess the validity of different implementations of the TDH method including the account of direct correlations between coordinate pairs, and mixed quantum-classical and quantum-Gaussian wave packets treatments. The latter yields very good results compared to the fully quantal treatment.

Q/C TDSCF

The mixed quantum/classical scheme is obtained by taking the classical limit of the equation in the R mode. This gives

$$\dot{p}_R = - \frac{\partial V_2^{\text{eff}}}{\partial R},$$

$$\dot{R} = \frac{p_R}{\mu_R},$$

where the $V_2^{\text{eff}}(R,t)$ is the same as before but $V_1^{\text{eff}}(r,t)$ is now constructed as a weighted sum over the classical trajectories.

$$V_1^{\text{eff}} = \frac{1}{n_T} \sum_{\alpha=1}^{n_T} V[r, R_\alpha(t)],$$

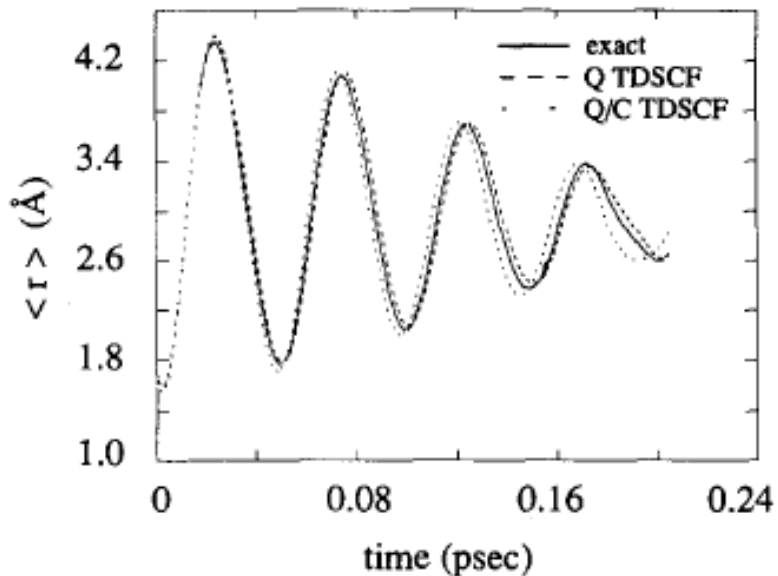


FIG. 5. The average interatomic HI distance as a function of time. Three results are superimposed. Note the small divergence of the Q/C TDSCF at the end.

MCTDH

Uwe Manthe and Hans D. Meyer

The multi-configurational time-dependent Hartree (MCTDH) approach [8,9] is ideally suited to facilitate numerically exact wave packet propagations under these circumstances. It then allows one to rigorously describe the quantum dynamics of polyatomic systems consisting of more than four or five atoms. The MCTDH approach employs a layered representation of the wavefunction

$$\psi(x_1, \dots, x_f, t) = \sum_{j_1=1}^{n_1} \dots \sum_{j_f=1}^{n_f} A_{j_1..j_f}(t) \prod_{\kappa=1}^f \phi_{j_\kappa}^{(\kappa)}(x_\kappa, t), \quad (4)$$

$$\phi_j^{(\kappa)}(x_\kappa, t) = \sum_{l=1}^{N_\kappa} c_{jl}^{(\kappa)}(t) \cdot \chi_l(x_\kappa).$$

$$\psi(x_1, \dots, x_f, t) = \sum_{j_1=1}^{n_1} \dots \sum_{j_f=1}^{n_f} A_{j_1..j_f}(t) \prod_{\kappa=1}^f \phi_{j_\kappa}^{(\kappa)}(x_\kappa, t), \quad (4)$$

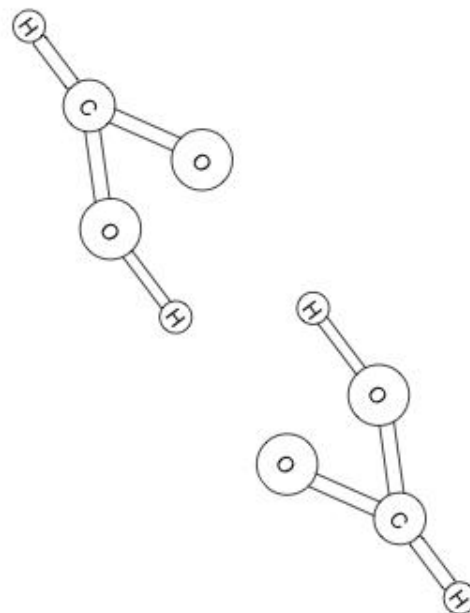
$$\phi_j^{(\kappa)}(x_\kappa, t) = \sum_{l=1}^{N_\kappa} c_{jl}^{(\kappa)}(t) \cdot \chi_l(x_\kappa).$$

The wavefunction is first represented in a basis of time-dependent expansion functions $\phi_{j_\kappa}^{(\kappa)}(x_\kappa, t)$ which are called single-particle functions. In a second layer of the representation, the single-particle functions are then represented in the basis of the underlying ‘primitive’ time-independent basis functions $\chi_l(x_\kappa)$. Standard discrete variable representation (DVR) [87–89] or fast Fourier transform (FFT) [90] schemes can be used to provide the $\chi_l(x_\kappa)$. The equations of motion which describe the expansion coefficients $A_{j_1..j_f}(t)$ and $c_{jl}^{(\kappa)}(t)$ of both layers can be obtained from the Dirac–Frenkel variational principle.

Double Proton Transfer Dynamics in Formic Acid Dimer

George Barnes and Ned Sibert

Previous Studies



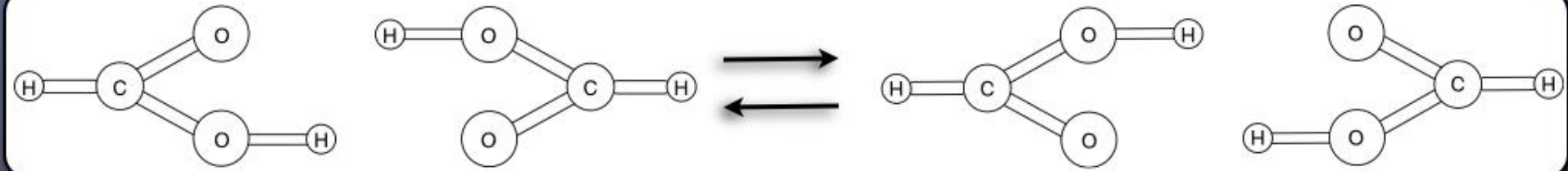
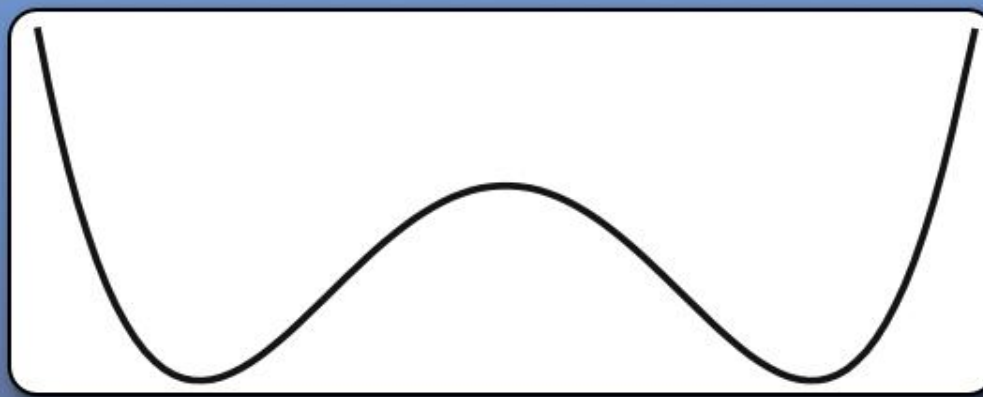
Experimental:

Madeja and Havenith JCP (2002)
Zielke and Suhm, PCCP (2007)
Pate, PCCP (2007)
Nibbering, CP (2007)

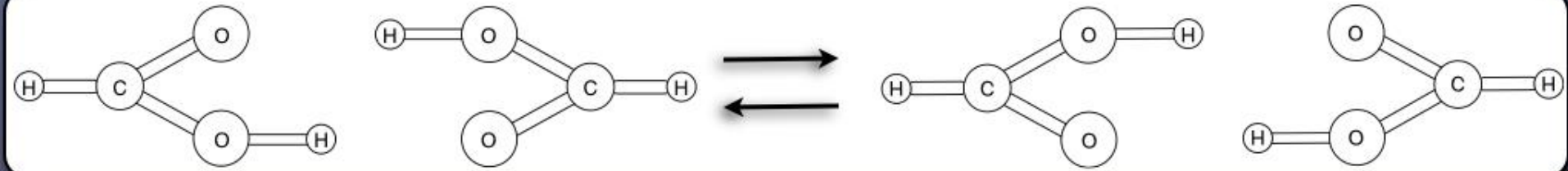
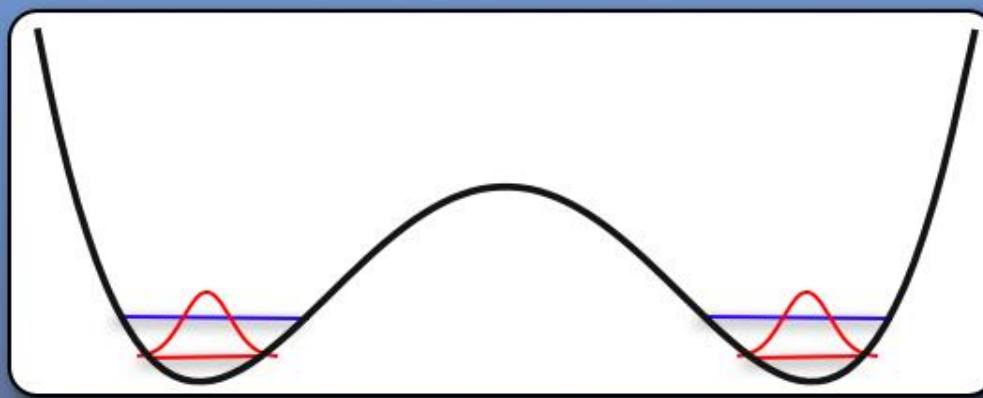
Theoretical:

Matanovic et al. JCP (2007)
Luckhaus JPCA (2006)
Mil'nikov et al. JCP (2005)
Smedarchina et al. JCP (2005)
Tautermann et al. JCP (2004)
Shida et al. JCP (1990)
Verner et al. CPL (1990)

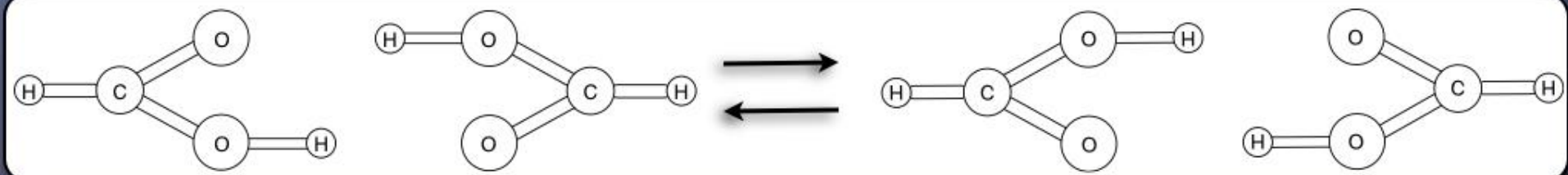
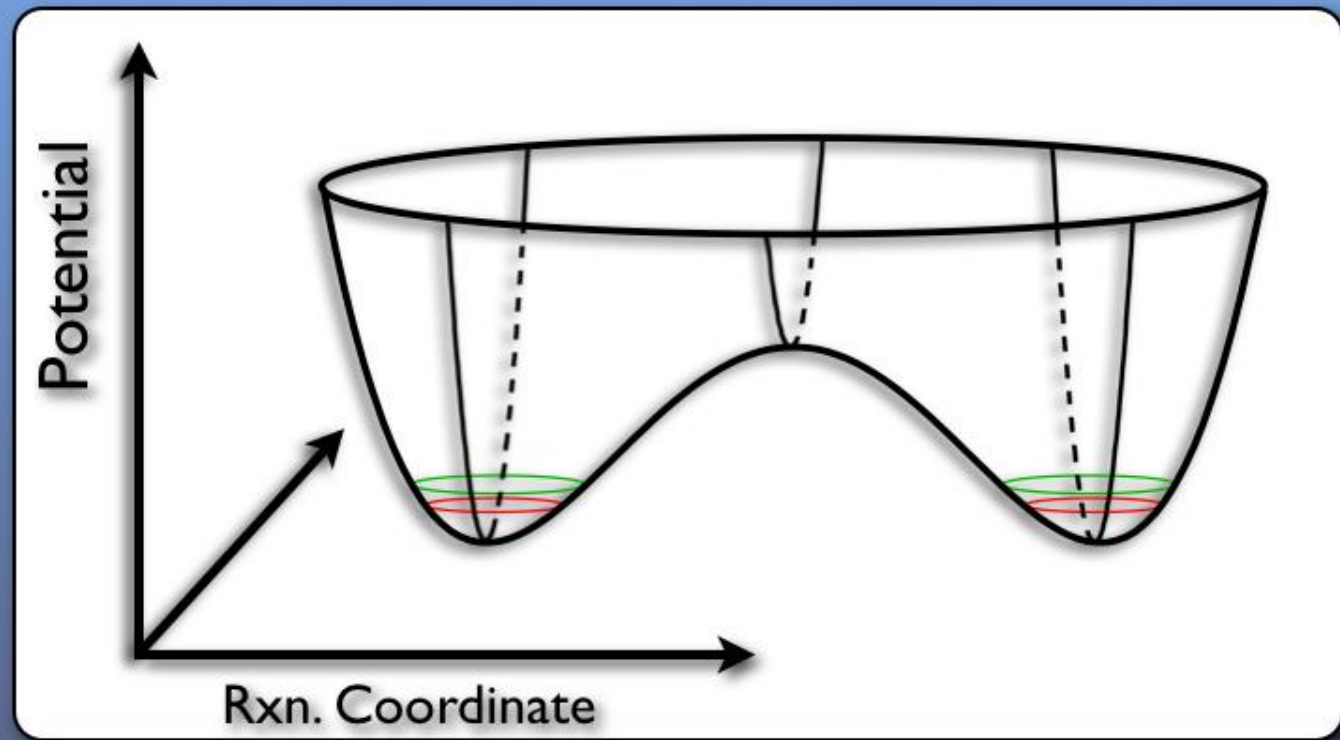
Formic Acid Dimer



Formic Acid Dimer



Reaction Surface Potential



The Model

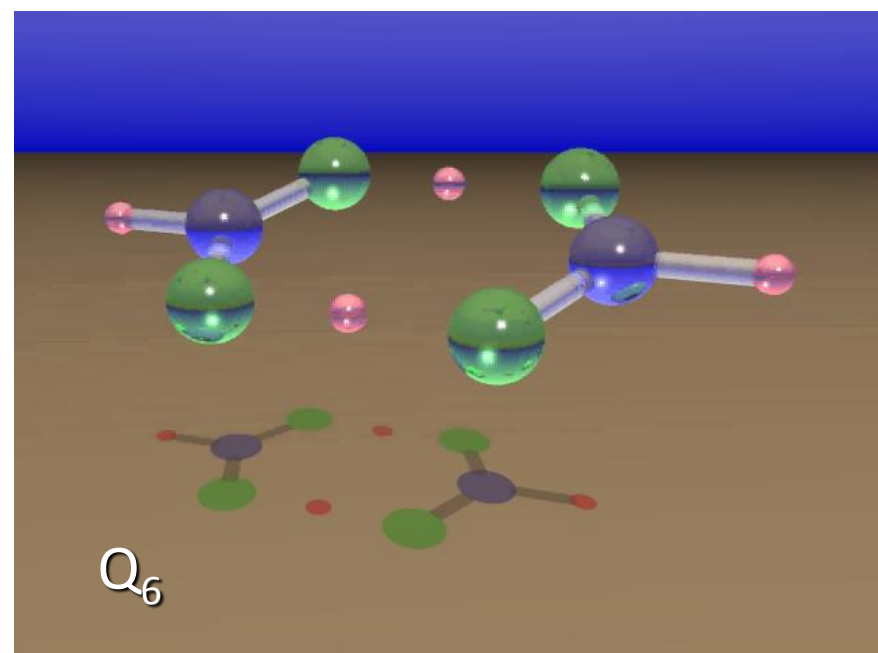
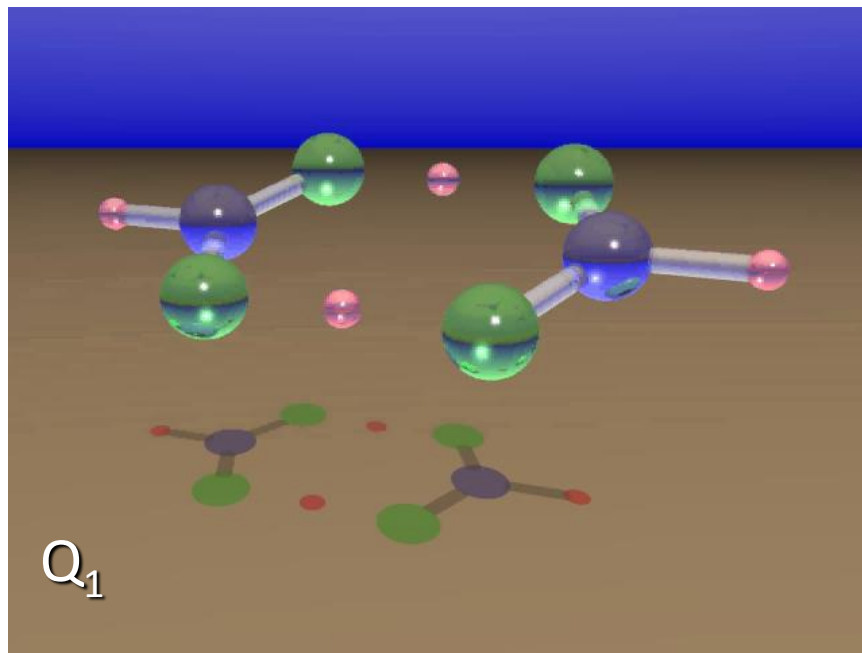
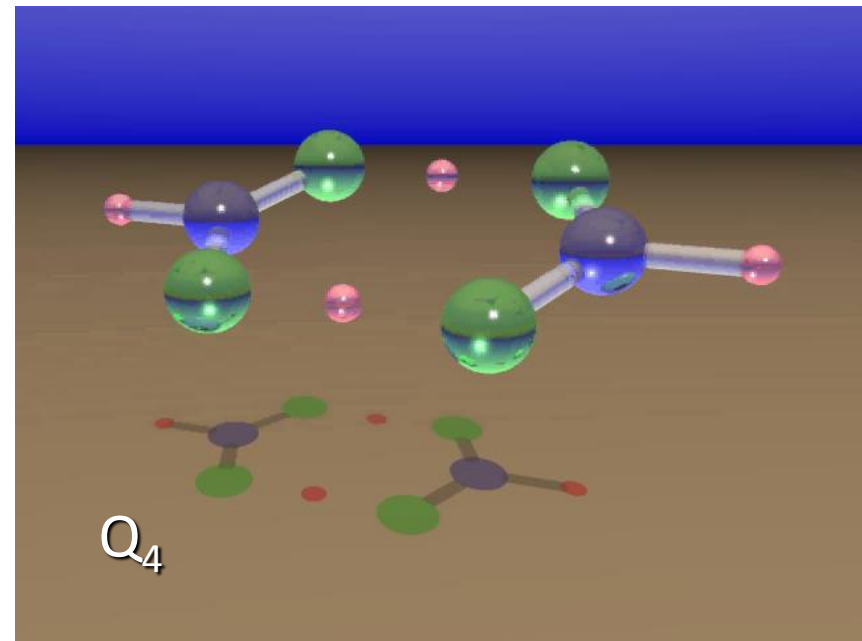
A model of double proton tunneling in formic acid dimer is developed using a reaction surface Hamiltonian.

The surface includes the symmetric OH stretch plus the in-plane stretch and bend inter-dimer vibrations.

The surface Hamiltonian is coupled to a bath of the remaining in-plane normal modes (except CH stretches) obtained at the D_{2h} transition state structure.

Important motions

These modes are 3 of the
TS normal modes

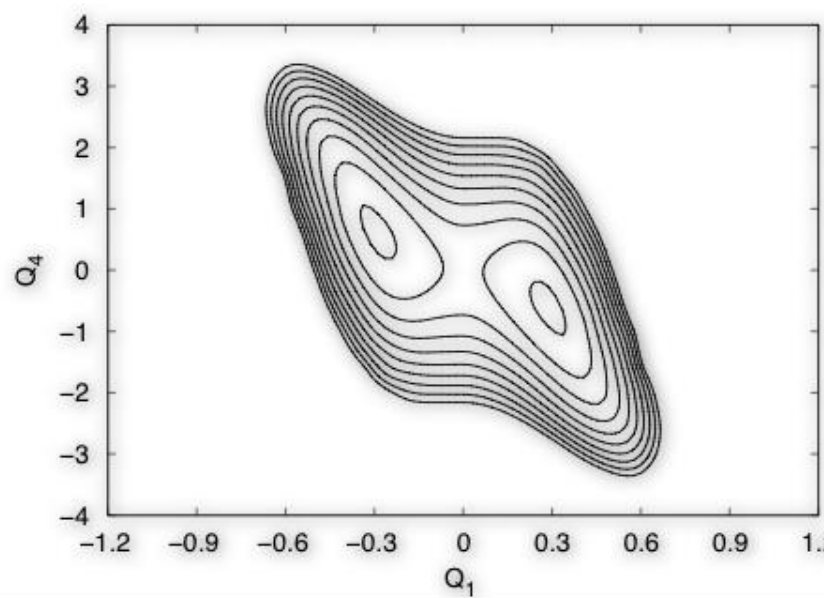
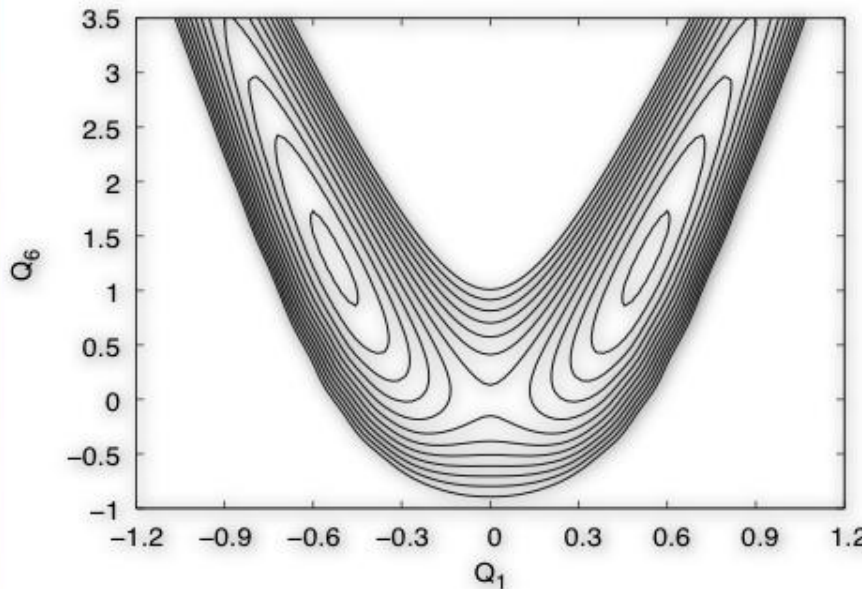


Think-Pair-Share Q

The relative importance of excitation of fundamentals of modes 1, 4, and 6 on increasing the tunneling splitting is

- A. 1>4>6
- B. 6>4>1
- C. 1>6>4
- D. I don't know.

The Potential

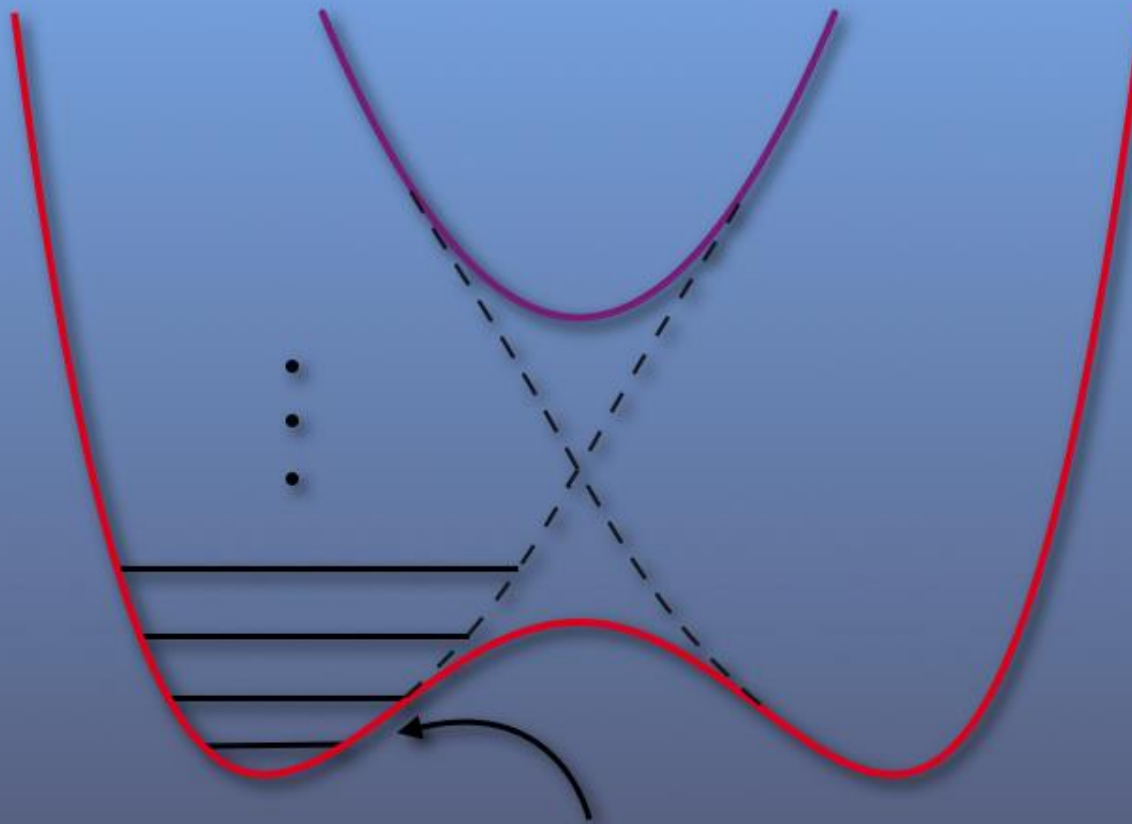


| Method | Barrier Height (cm^{-1}) |
|-----------------|-------------------------------------|
| G3 | 2871 |
| G2 | 3091 |
| B3LYP/6-31G+(d) | 2917 |

Tautermann, et al. J. Chem. Phys. **120**, 11650
Loerting, et al. J. Chem. Phys. **120**, 12595

Goal is to solve for the eigenfunctions of these 3 dimensions.

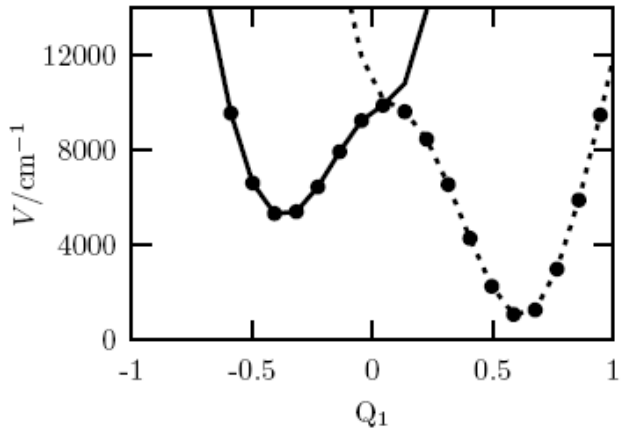
Diabatic Decomposition



OH Stretch Functions

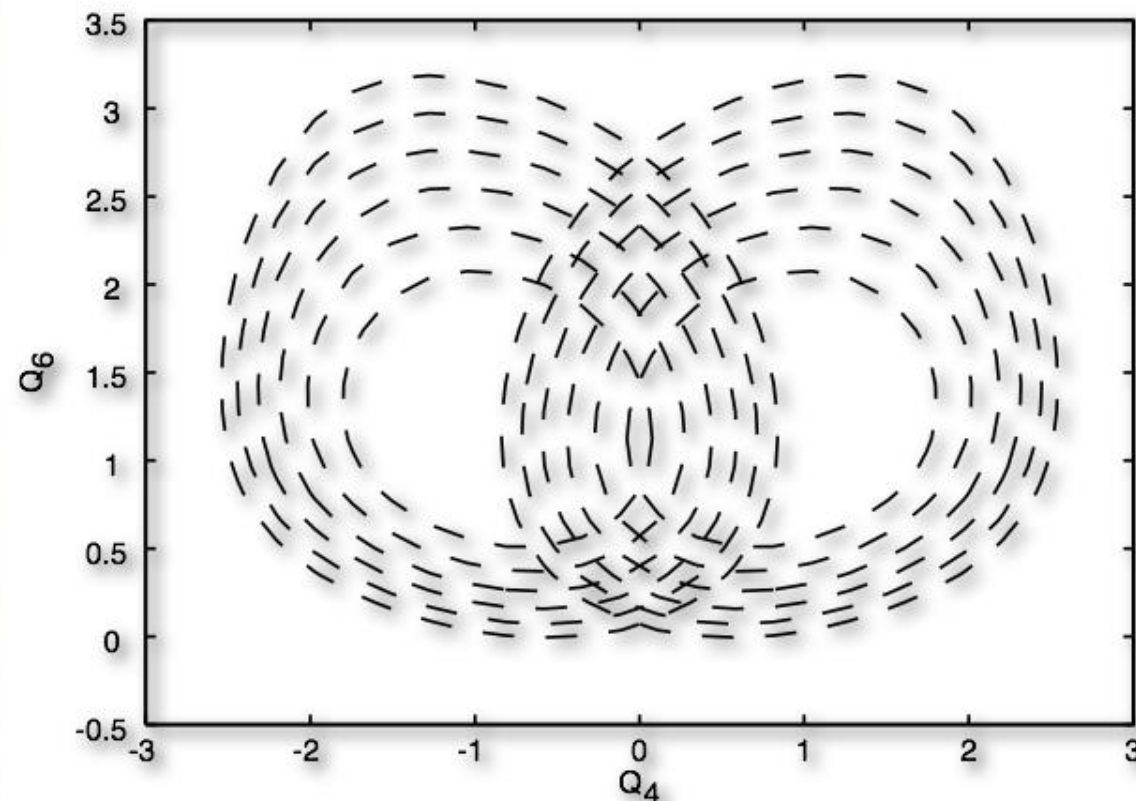
Diabatic Approach

$$\begin{pmatrix} V_L^0 & W \\ W & V_R^0 \end{pmatrix} \begin{pmatrix} \Psi_L \\ \Psi_R \end{pmatrix} = E_{\pm} \begin{pmatrix} \Psi_L \\ \Psi_R \end{pmatrix}.$$



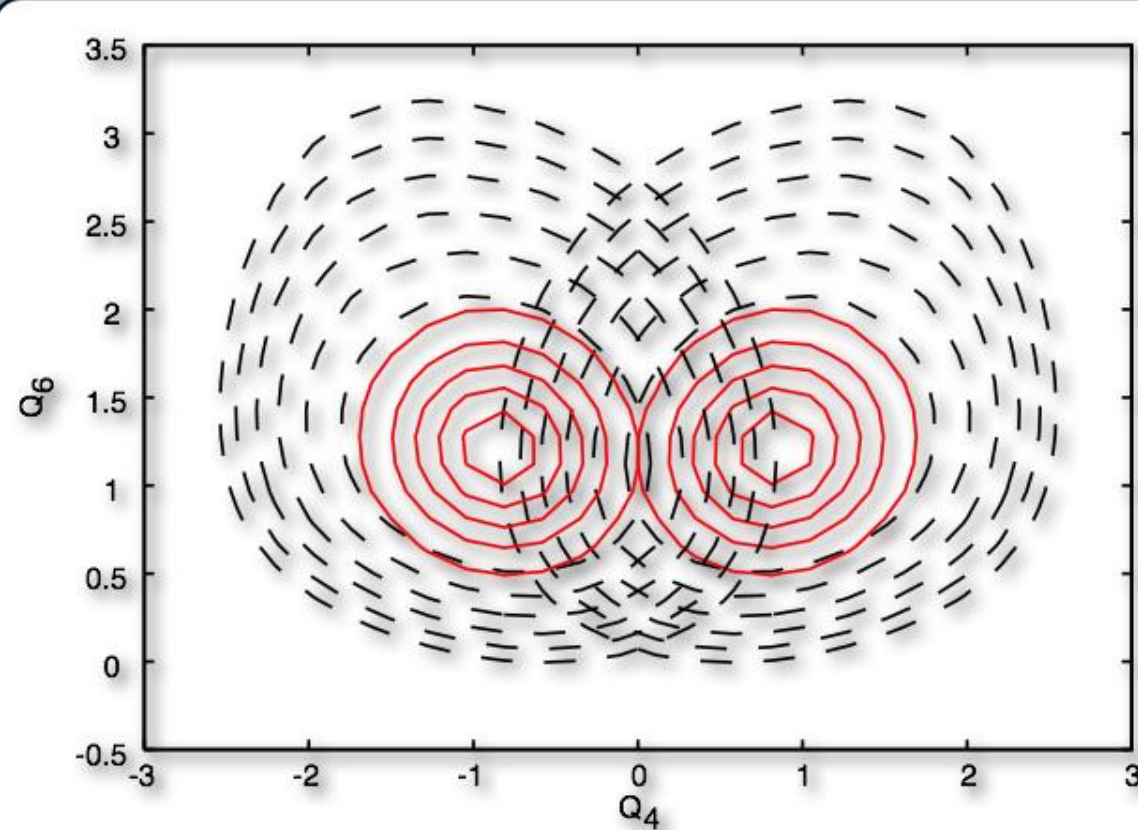
$$\left[\frac{P_1^2}{2} + V_L^0(Q_1, Q_{4j}, Q_{6k}) \right] |j_1^{j,k}, L\rangle = E_{j_1}^L(Q_{4j}, Q_{6k}) |j_1^{j,k}, L\rangle$$

Diabatic Representation

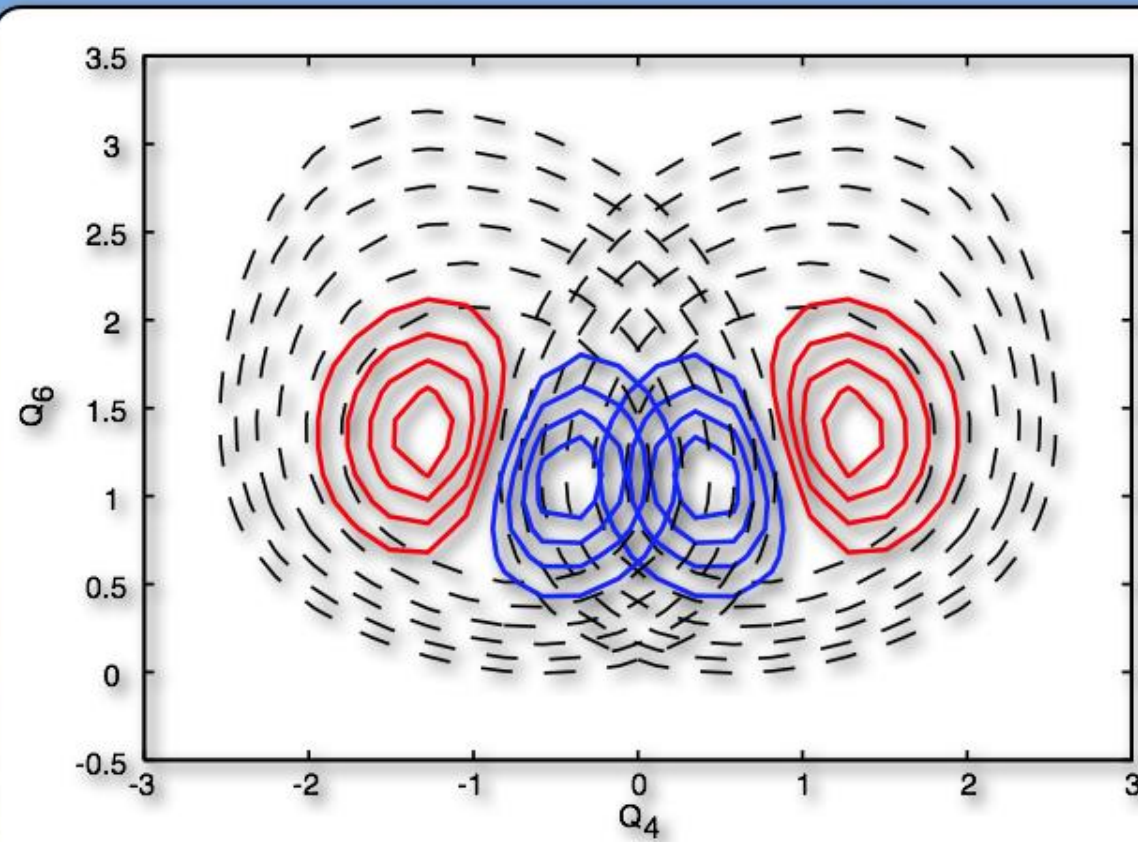


The OH Stretch Surface

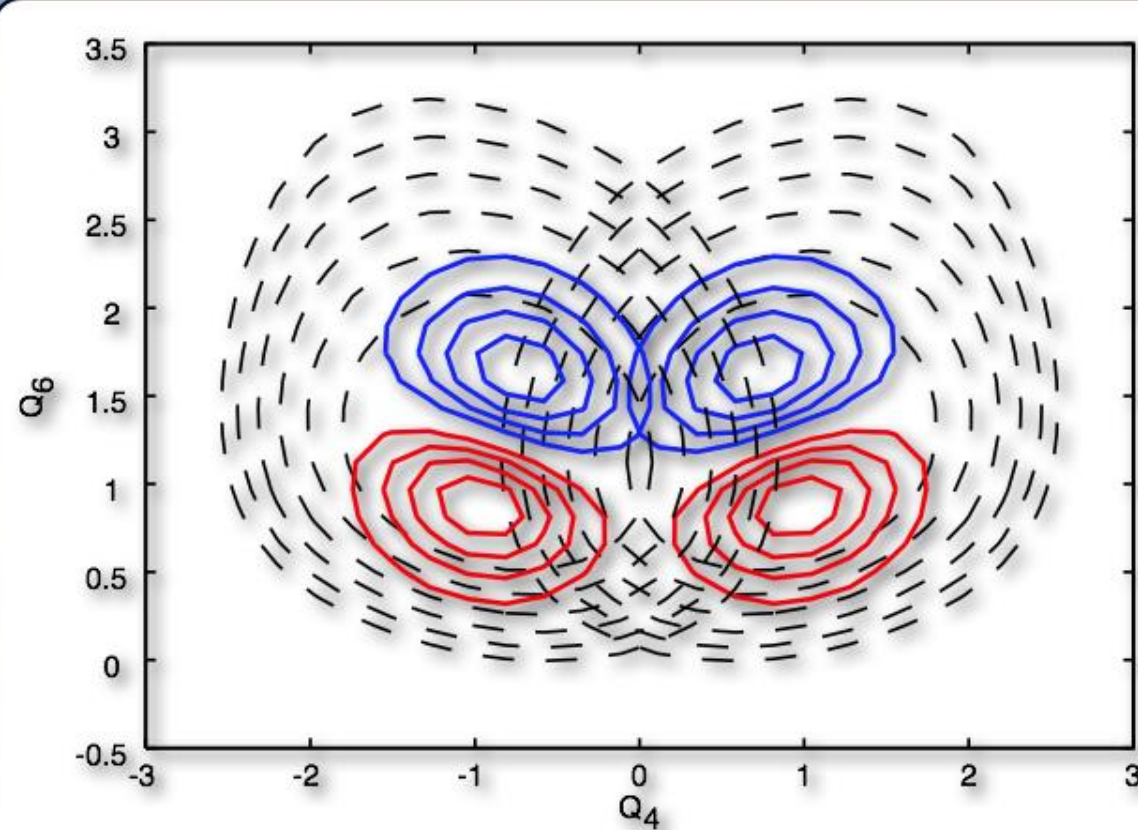
Diabatic Representation



Diabatic Representation



Diabatic Representation

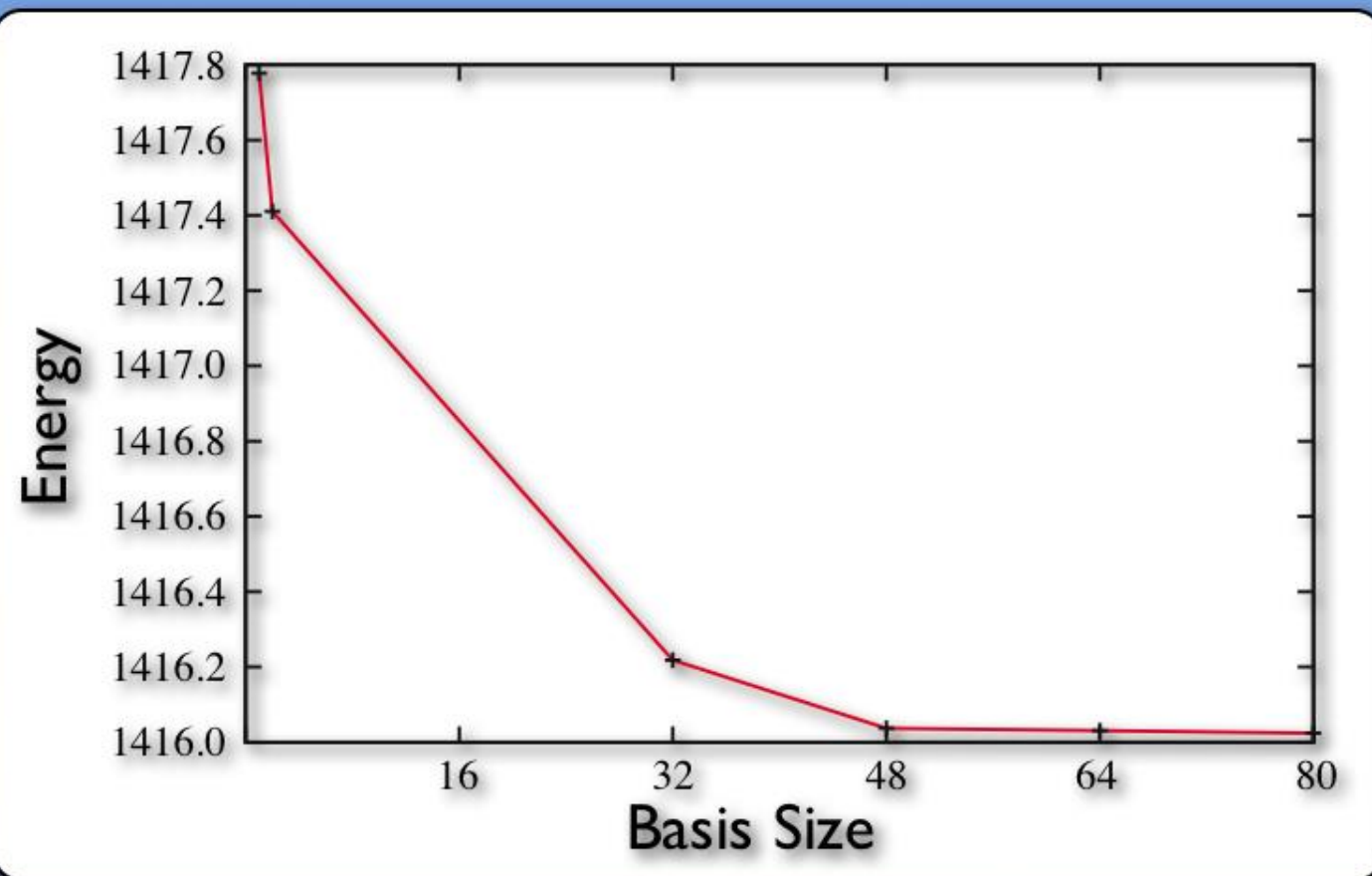


Think-Pair-Share Q

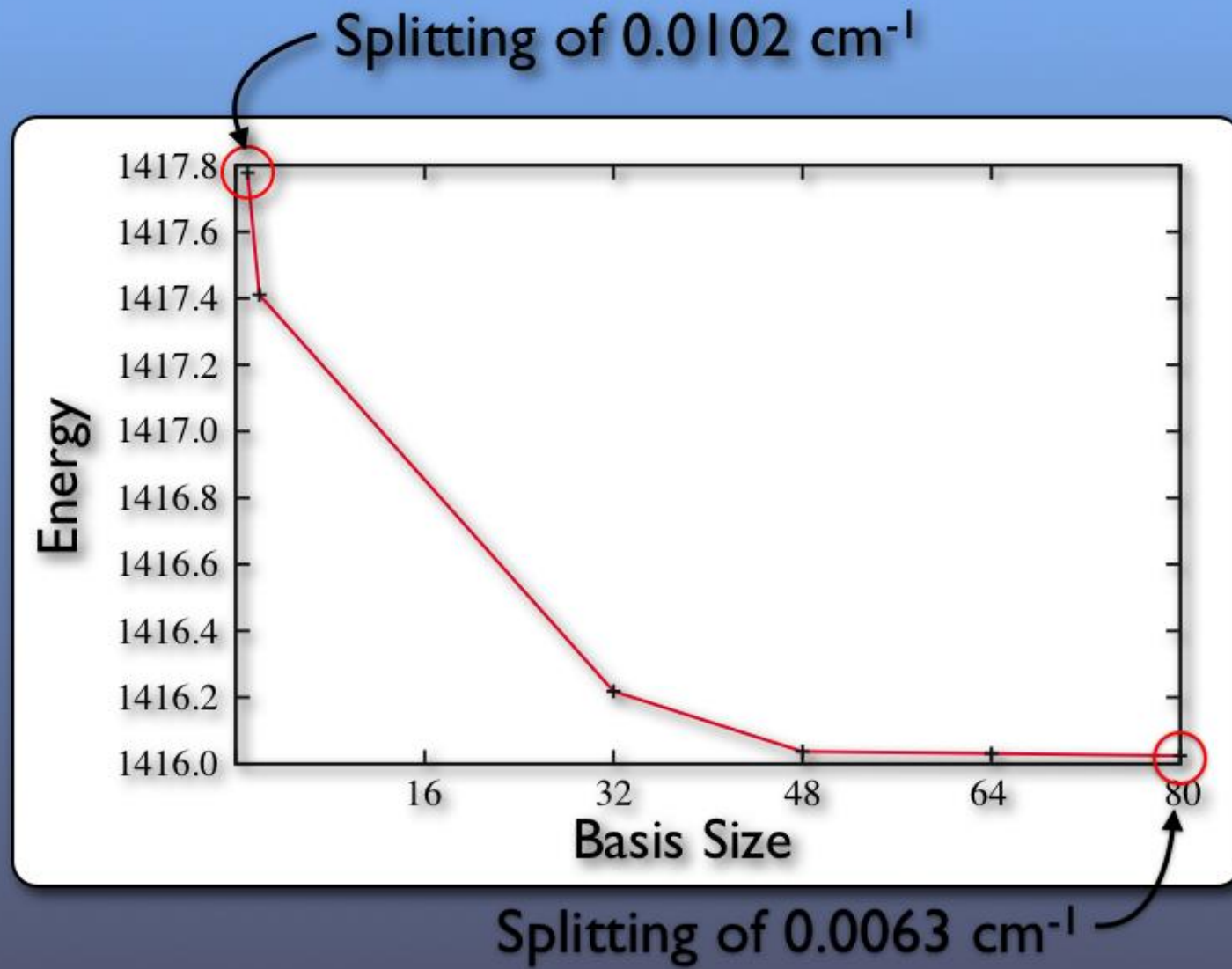
The relative importance of excitation of fundamentals of modes 1, 4, and 6 on increasing the tunneling splitting is

- A. 1>4>6
- B. 6>4>1
- C. 1>6>4
- D. I still don't know.

Reaction Surface Convergence



Reaction Surface Convergence



Select eigenvalues for the RS Hamiltonian obtained with the {4,40} basis

| state | ω | Δ | n_1 | n_4 | n_6 |
|-------|----------|----------|-------|-------|-------|
| 1 | 0.000 | 0.006 | 0 | 0 | 0 |
| 2 | 166.232 | 0.052 | 0 | 1 | 0 |
| 3 | 211.717 | 0.007 | 0 | 0 | 1 |
| 4 | 333.505 | 0.218 | 0 | 2 | 0 |
| 5 | 375.326 | 0.064 | 0 | 1 | 1 |
| 6 | 419.961 | 0.004 | 0 | 0 | 2 |
| 7 | 502.466 | 0.569 | 0 | 3 | 0 |
| 8 | 540.364 | 0.300 | 0 | 2 | 1 |
| 9 | 581.292 | 0.042 | 0 | 1 | 2 |
| 10 | 625.204 | 0.002 | 0 | 0 | 3 |
| 11 | 673.209 | 1.038 | 0 | 4 | 0 |
| 12 | 707.287 | 0.930 | 0 | 3 | 1 |
| 13 | 744.521 | 0.192 | 0 | 2 | 2 |
| 14 | 784.501 | 0.017 | 0 | 1 | 3 |
| 15 | 827.585 | 0.001 | 0 | 0 | 4 |
| 41 | 2223.484 | 11.348 | 1 | 0 | 0 |

Conclusion

- Using DVR combined with diabatic wave functions provides an efficient way to calculate and interpret tunneling splittings.
- Mode 4 has the same role as the solvent.